Diverse and durophagous: Early Carboniferous chondrichthyans from the Scottish Borders

Kelly R. Richards[1*], Janet E. Sherwin[2], Timothy R. Smithson[1], Rebecca F. Bennion[1**], Sarah J. Davies[2], John E. A. Marshall[3] and Jennifer A. Clack[1]

[1] University Museum of Zoology, Cambridge, Downing Street, Cambridge CB2 3EJ, UK.
[2] School of Geography, Geology and the Environment, University of Leicester, University Road, Leicester LE1 7RH, UK.
[3] Ocean and Earth Science, University of Southampton, National Oceanography Centre, European Way, Southampton SO14 3ZH, UK.
[*] Current address: University of Oxford Museum of Natural History, Parks Road, Oxford, OX3 1PW, UK.
[**] Current addresses: (1) Geology Research Unit, Université de Liège, 14 Allée du 6 Août, 4000 Liège, Belgium. (2) Directorate of Earth and History of Life, Royal Belgian Institute of Natural Sciences, 29 rue Vautier, 1000 Brussels, Belgium.

ABSTRACT: Chondrichthyan teeth from a new locality in the Scottish Borders supply additional evidence of Early Carboniferous chondrichthyans in the UK. The interbedded dolostones and siltstones of the Ballagan Formation exposed along Whitrope Burn are interpreted as representing a restricted lagoonal environment that received significant amounts of land-derived sediment. This site is palynologically dated to the latest Tournaisian–early Viséan. The diverse dental fauna documented here is dominated by large crushing holocephalan toothplates, with very few, small non-crushing chondrichthyan teeth. Two new taxa are named and described. Our samples are consistent with worldwide evidence that chondrichthyan crushing faunas are common following the Hangenberg extinction event. The lagoonal habitat represented by Whitrope Burn may represent a temporary refugium that was host to a near-relict fauna dominated by large holocephalan chondrichthyans with crushing dentitions. Many of these had already become scarce in other localities by the Viséan and become extinct later in the Carboniferous. This fauna provides evidence of early endemism or niche separation within European chondrichthyan faunas at this time. This evidence points to a complex picture in which the diversity of durophagous chondrichthyans is controlled by narrow spatial shifts in niche availability over time.

KEY WORDS: Ballagan Formation, post-Hangenberg, teeth, Tournaisian.

Chondrichthyan evolutionary history is dominated by two radiations. The first, Palaeozoic, radiation reached peak diversity during the Viséan of the Early Carboniferous and by the end of the second, Mesozoic, radiation all of the modern Neoselachian families were in evidence (Underwood *et al.* 1999; Kriwet *et al.* 2009). Body fossils of chondrichthyans are rare and our understanding of the pattern and timing of the Palaeozoic radiation is based on a mixture of isolated teeth and body fossils from a small number of mid-Carboniferous lagerstätten. Prior to the Viséan (Sallan & Coates 2010) fossil evidence of chondrichthyans is relatively scarce. Devonian chondrichthyans comprise only a small proportion of a fauna dominated by sarcopterygians and placoderms. Chondrichthyans are the dominant marine group by the Viséan, with actinopterygians promoted to second place in the absence of placoderms and a decline in sarcopterygian diversity (Sallan & Coates 2010). The Hangenberg extinction event (HEE) may have driven the Palaeozoic radiation through the provision of vacated niche space and environment alteration. However, there have been a few chondrichthyan fossils documented from the Tournaisian which could provide evidence for a chondrichthyan radiation directly succeeding the event. The 15 million-year Tournaisian timespan between the HEE and peak chondrichthyan diversity in the Viséan, known as 'Romer's Gap', is famous for its lack of vertebrate fossils generally. Body fossils of chondrichthyans are non-existent and evidence is confined to isolated teeth, scales and spines.

Tournaisian chondrichthyans are scattered over a number of regions, including the UK (Wood & Rolfe 1985; Schram 1979) and Ireland (Duncan 2003, 2004, 2006); Germany (Ginter 1999); Russia (Lebedev 1996); the southern Urals (Ivanov 1996); Alberta (McKenzie & Bamber 1979); Nova Scotia (Manski & Lucas 2013); Australia (Roelofs *et al.* 2016; Turner 1982, 1991, 1993; Garvey & Turner 2006) Iran (Habibi & Ginter 2011); southern China (Ginter & Sun 2007); and the mid-west USA (Newberry & Worthen 1866; St John & Worthen 1875, 1883). Definitively Tournaisian chondrichthyans in the UK are represented by just six genera: *Lophodus* from Foulden (Wood & Rolfe 1985); *Helodus* from Coomsdon Burn (Schram 1979); and *Cladodus*, *Helodus*, *Chomatodus*, *Psammodus* and *Orthacanthus* from the Avon Group (Stoddart 1875).

An additional, much more diverse, fauna is from the Black Rock Limestone Subgroup localities. The first fauna includes those found in the Avon Group, with the addition of *Orodus*, *Ctenacanthus*, *Cochliodus*, *Tomodus*, *Deltoptychius* and additional species of *Helodus* and *Cladodus* (Stoddart 1875). The second is found in the Black Rock Limestone of Cromhall Quarry and is, unusually so far, dominated by non-holocephalan

 doi:10.1017/S1755691018000166

chondrichthyans and documents sixteen taxa, only three of which are holocephalan (Behan *et al.* 2012). In this paper, we describe an additional Tournaisian chondrichthyan fauna from a new northern UK site. Unlike the previous records, with the possible exception of the Bristol localities documented by Stoddart, this is interpreted as a shallow, near-shore marine site. High-resolution geological analysis shows that the deposit is likely to be lagoonal and the vertebrate remains have been concentrated by intra-lagoonal currents and density flows. This locality represents a rare opportunity to link Tournaisian chondrichthyan remains with fine-scale palaeoenvironmental evidence and expands the range of environments known from the Tournaisian. We document the high chondrichthyan diversity and show how this fauna contributes to our understanding of the timing and pattern of post-HEE chondrichthyan recovery and radiation.

Institutional abbreviations. BGS, British Geological Survey; BRSUG, Bristol University, School of Earth Science collection, Bristol; NHMUK, Natural History Museum, London; NMS, National Museums Scotland, Edinburgh; UMZC, University Museum of Zoology, Cambridge; UoL, University of Leicester.

1. Geological setting

1.1. Location and stratigraphic context

During the Early Carboniferous, the Whitrope Burn site was located close to the northern edge of the Northumberland Basin and to the west of the Cheviot Block (Stone *et al.* 2010). The Northumberland Basin is a half-graben with up to 5000 m of synrift sediments adjacent to the southern margin (Stone *et al.* 2010). The strata at Whitrope Burn (Near Hawick, GR [NY507 965]) are part of the Ballagan Formation deposited during the Tournaisian, within the upper Inverclyde Group. The Ballagan Formation is characterised by inter-bedded sandstones, mudstones, and argillaceous dolostones ('cementstone') deposited in lacustrine to lagoonal environments, with occasional marine incursions from a seaway to the west (Stone *et al.* 2010).

1.2. Sedimentology

The section preserving the diverse fauna of chondrichthyans exposed at Whitrope Burn is 70 cm in thickness (Fig. 1) and is part of a partially exposed succession of alternating packages of dolostones (dolomite-cemented limestones) and thick siltstones/mudstones. See Figure 2 for cut rock surface images.

At the base of the succession is a series of four, thin (5–7 cm) dolomite-cemented, fining-upward limestone beds with undulose laminae (Fig. 1, beds 1–4). Each bed contains lithic clasts (generally 1–3 mm in size but, in the lowest bed, up to 2 cm in size) and has a micritic dolomite top. The carbonate mud clasts, some of which are laminated, are suspended in a matrix composed mainly of micritic dolomite, with quartz and larger calcite grains (typically fine sand-sized) and some fossil fragments (Fig. 2a, b). The micrite comprises euhedral to subhedral rhombs of dolomite (2–10 μm) in a clay matrix. Fossil fragments are common, but not abundant, in these lower beds and include plant material (up to 8 mm), shelly fragments including occasional incomplete ostracods, a few actinopterygian teeth and some small bone and scale fragments. Fossil material is more abundant in the basal part of the topmost bed, and this bed also has a thicker micrite cap.

These thin beds are interpreted as calciturbidites: erosive flows, derived from the margin of the basin, transported and concentrated material below wave-base. The multiple internal erosional surfaces suggest repeated relatively small surges of slightly coarser material within the main flow. The undulose

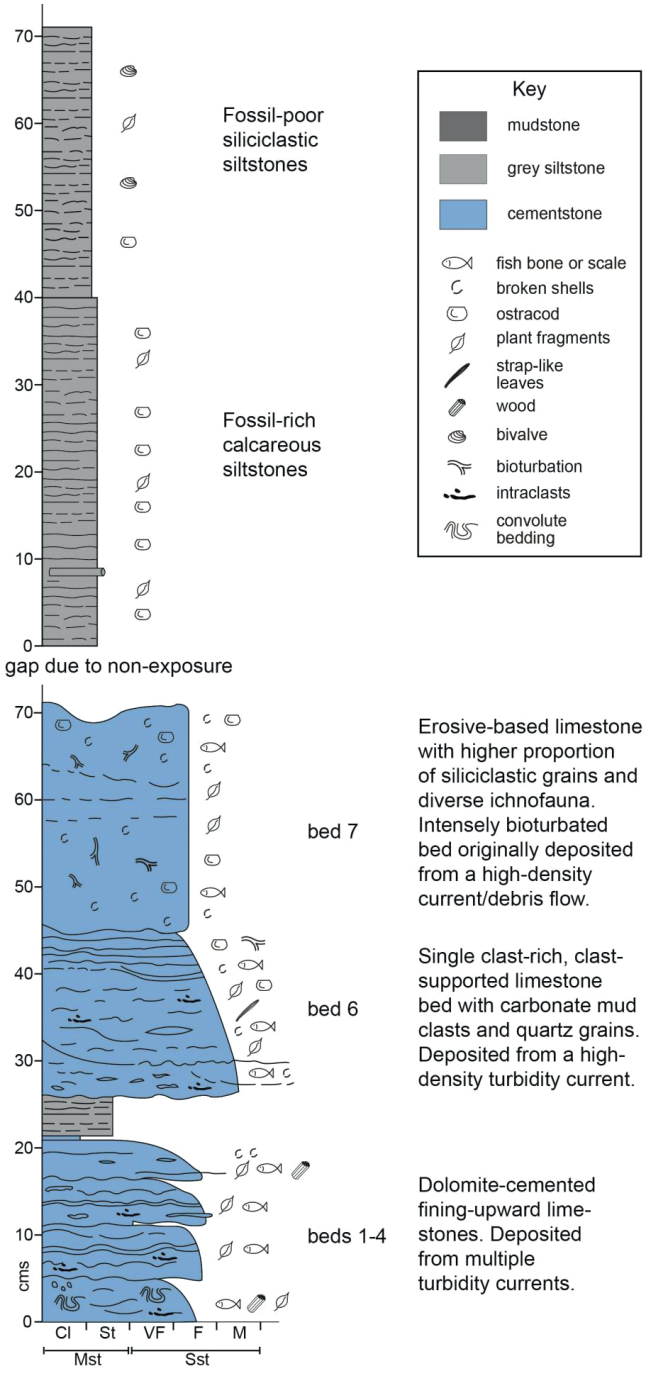

Figure 1 Sedimentary log and interpretation of the section at Whitrope Burn. Bed 6 is the main chondrichthyan-bearing bed.

internal laminae may be the result of soft-sediment deformation and/or deposition onto a very soft substrate deposited by the earlier flow.

The thicker carbonate mud top to the uppermost bed may indicate either a prolonged period of settling of the tail end of the flow, or carbonate precipitation from the water column, before the deposition of the overlying richly fossiliferous bed and an intervening thin (4 cm) siltstone.

The key bed occurs 26 cm above the base of the section and has a particularly rich and diverse assemblage of cartilaginous and bony fish and some tetrapod remains. This 20-cm bed (bed 6) is clast rich and clast supported with a matrix of fine-medium quartz and calcite grains mixed with a carbonate mud (Fig. 2c). Although larger clasts (0.5–1 cm) typically occur near the bed base overall the clasts appear unsorted. The diverse clast assemblage includes lithic fragments, strap-like plant leaves (5–10 cm wide), well preserved vertebrate fossil

https://doi.org/10.1017/S1755691018000166 Published online by Cambridge University Press

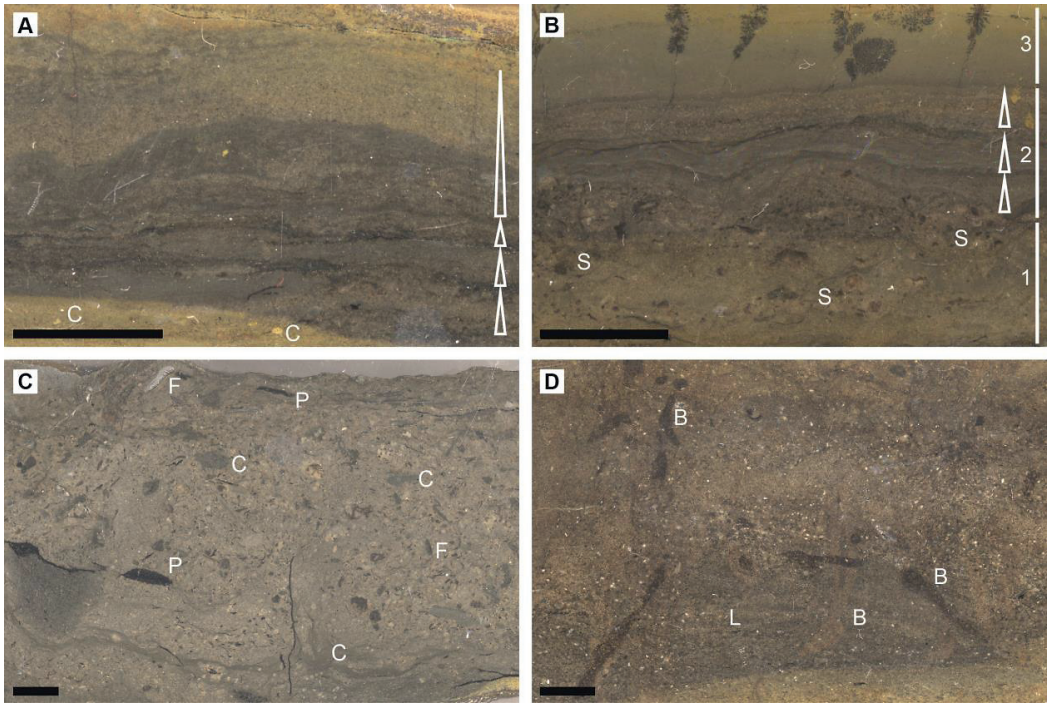

Figure 2 Sedimentological images for facies analysis. (A) UoL/D/15/007/WB14-04-03. Lower, thin bed, showing small fining upward beds (arrows), transported lithic clasts, undulating nature of the laminae, and general fining upward. (B) UoL/D/15/007/WB14-04-02. Lower, thin bed, illustrating the coarse bed base, (with shells, occasional ostracods, scale fragments and small plant material), and overlying fining-upward laminae, soft sediment deformation, and very fine top. Part 1 is a mixed, unsorted layer containing bioclastic material; part 2 is a laminated section, arising from pulsed, coarser inputs within the flow; part 3 is very fine carbonate material representing deposition from the finest part of the flow, or precipitation of micrite from the water column. (C) UoL/D/15/007/WB14-04-06. Bed 6, showing chondrichthyan material (F), mud clasts and plant material. (D) UoL/D/15/007/WB14-04-07. Bed 7, bioturbated, with some remnant lamination (L) and burrows. Key to labels: B = burrow; C = transported lithic clasts; F = fish fragment; L = laminae; P = plant material; S = shelly fragments. Scale bars = 1 cm.

fragments (including toothplates, remains of cartilaginous and bony fish, and some tetrapod fragments) and shelly material (predominantly ostracods and serpulids). The cartilaginous fish remains are the subject of this paper. The complex internal structure of the bed is characterised by multiple erosion surfaces that are overlain by fine-grained laminae. Each erosive surface is associated with abundant clasts, and concentrations of toothplates and other fossil material.

The limited sorting of this bed might indicate a debris deposit, but its clast-supported character and a slight upward fining is interpreted as deposition from a high-density turbidity current, where the flow concentrated fossil material and mixed it with carbonate mud, but did little in the way of sorting. The finer-grained laminae towards the top were probably deposited as part of the waning flow. Large strap-like plant leaves indicate that the origin of flow must have been relatively close to shore, or that the large plant material was temporarily stored on the shelf before being transported into the deeper water and more distal reaches of a lagoon.

Overlying the fossiliferous bed is a bioturbated dolomite-cemented limestone, with an erosive base and greater siliciclastic content (bed 7). This 25-cm bed has been intensively bioturbated, with an ichnofauna that includes *Teichichnus* (Bromley 1996; Pemberton *et al*. 2001), but retains some remnant lamination (Fig. 2d). Fossil fragments are common, although not abundant, and comprise ostracods, lungfish material (Smithson *et al*. 2015) bone and scale fragments, and small (1–2 mm) pieces of plant and megaspores. Fossil fragments do not appear crushed, and many are pyritised. Cavity-filling kaolinite and distributed barite are observed.

The more abundant siliciclastic material suggests an increase in land-derived sediment. This bed may have been deposited by similar processes as the underlying units, but the bioturbation has removed much of the internal structure suggesting that, after deposition, there was time to colonise the sediment. The presence of *Teichichnus* supports a shoreface to offshore environment (Pemberton *et al*. 2001). The minimal compaction of fossil fragments and burrows suggests early lithification with the products of diagenesis, namely pyrite, kaolinite and barite.

The limestone beds are overlain by at least 70 cm of micaceous siltstones. The lower, 40 cm thick, siltstones are bedded, contain carbonate and are fossil rich (Fig. 1). Small ostracods (0.5–1 mm), considered to be juveniles, are abundant and are sometimes concentrated into masses with spirorbiform worm tubes. Small pieces of plant and spore material are also common.

The upper siltstones are less well-bedded, do not contain carbonate, and are at least 30 cm thick; the top is unseen. Plant material is small (up to 8 mm) but common; rare ostracods, all *Cavellina* ?sp., and some bivalves (*Naiadites*) are present, but none have retained shells.

The presence of siltstone indicates an increase in silt- and clay-sized siliciclastic material delivered to this part of the basin that may have induced a switch-off in carbonate production. The upper siltstones do not contain carbonate, indicating that carbonate production ceased.

The abundant, sometimes concentrated, juvenile ostracods of the lower siltstones may indicate winnowing, or that localised conditions were not conducive to permanent ostracod development. The occasional *Cavellina* ?sp. ostracods found in the upper siltstones are a eurytopic species (Williams *et al*. 2006; Bennett *et al*. 2012). In the nearby Roughley Burn, the bivalve *Naiadites* is associated with the marine species *Sanguinolites* (Edwards & Stubblefield 1947; Brandon *et al*. 1995) in the

https://doi.org/10.1017/S1755691018000166 Published online by Cambridge University Press

equivalent succession. The combination of *Cavellina* ?sp. and *Naiadites* at Whitrope Burn suggests a marine environment for the Whitrope Burn site.

1.3. Age of Whitrope Burn

Palynological analysis of the Whitrope Burn succession shows that it is likely to lie within the latest Tournaisian to early Viséan age interval. This is based on the presence of the spore *Lycospora noctuina*, a species that parallels *L. pusilla* in range. The inception of *L. pusilla* has been used to define the base of the Viséan. However, there is no secure pick that links its inception to the nominated Viséan global boundary stratotype section and point (GSSP), where its base will ultimately be defined by the within-lineage inception of the foraminifera *Eoparastaffella simplex*. Reviews from a compilation of data across Europe (e.g., Turnau *et al*. 1997) indicate a consistent synchronous inception of *L. pusilla* in the latest Tournaisian. As these palynological samples are spot samples from a single locality, rather than a continuous series of samples, there is no defined within sequence inception of *Lycospora* spp. However, the low numbers present indicate a position close to its range base and somewhere within the latest Tournaisian to early Viséan interval. *Schopfites claviger*, *Auroraspora macra* and *Plicatispora scolecophora* are also found in low numbers.

2. Materials and methods

2.1. Collection

The Whitrope Burn site was discovered in 2006 by Stan Wood. A large number of chondrichthyan teeth were collected at that time by him and are accessioned to the National Museum of Scotland (NMS). Tim Smithson and Jenny Clack visited the site later that year with Stan and collected further material. These specimens are accessioned to the University Museum of Zoology, Cambridge (UMZC). In 2014, Tim Smithson, Becky Bennion, Kelly Richards and Rob and Jenny Clack added to the UMZC collection and Nick Fraser and Andy Ross added to the NMS collection. Janet Sherwin logged and sampled the section in 2014.

2.2. Geological analysis

A total of 1.4 metres was logged in two sections at a centimetre scale. The base of the section is not visible, and the two sections are separated by an unexposed area. Ten samples were taken. Six of these hand specimens were cut and ground to give a smooth surface and reveal the internal fabric; the surfaces were then scanned. Polished ultra-thin sections (20 μm thick) were made from four of these samples and these were examined using an Olympus petrographic microscope. Two samples (UoL/D/15/007/WB14-04-02 and UoL/D/15/007/WB14-04-07) were treated with a 10 % solution of HCL, and rinsed using de-ionised water, to extract all the carbonate so that the percentage of non-carbonate residue could be determined. Samples UoL/D/15/007/WB14-04-01, UoL/D/15/007/WB14-04-02, UoL/D/15/007/WB14-04-03, UoL/D/15/007/WB14-04-04 and UoL/D/15/007/WB14-04-07 were examined on a Hitachi S-3600N environmental scanning electron microscope, and an Oxford INCA 350 EDX system was used to determine the elements present. XRD analysis was completed on three samples (UoL/D/15/007/WB14-04-01, UoL/D/15/007/WB14-04-02, UoL/D/15/007/WB14-04-07), using a Bruker D8 advance diffractometer. Specimens UoL/D/15/007/WB14-04-05, UoL/D/15/007/WB14-04-06, UoL/D/15/007/WB14-04-08, UoL/D/15/007/WB14-04-09 and UoL/D/15/007/WB14-04-010 were examined, with no preparation, using a Leica S6E binocular microscope.

2.3. Palynological analysis

The sample was lightly crushed to fragments a few mm in size. A 5g sample was then treated with 30 % HCl to remove carbonates and, particularly, any Ca^{2+} that would react with the HF to form an insoluble patina on the fragments. Following decant washing to neutral, the sample was then demineralised with 60 % HF, again followed by decant washing to neutral. It was then sieved at 15 μm and the coarser fraction treated in hot 30 % HCl to solubilise any neoformed fluorides. The sample was quickly diluted in water and resieved before being stored in a vial. Examination showed that the samples were dominated by large plant fragments. These were removed by top-sieving at 150 μm. The small size fraction was then mounted in Elvacite 2044. No oxidation methods were employed, as the palynomorphs were generally pale in colour.

2.4. Fossil preparation

Specimens were prepared using a combination of acetic acid and mounted-needle preparation. Specimens that were acid prepared were immersed in 5 % acetic acid for 24 hours with calcium phosphate buffer. Specimens were rinsed through three-hourly water changes for the subsequent three days. Loose sediment samples were filtered through filter paper so that all fractions were retained, dried overnight and picked using a Nikon SMZ-2B binocular light microscope. Photographs were taken with a Canon EOS 5D and tripod. Photos were prepared for plates in Photoshop v11.0.2. Photo stacking was used to increase the depth of field of images of the smallest teeth. A number of specimens were micro-CT-scanned using the UMZC X-tek micro-CT Scanner at resolutions of between 5 μm and 7 μm. The scan data were processed using Mimics V14 and segmented using multiple slice threshold editing techniques. The resultant 3D models were rendered using Meshlab v1.3.4 and Blender v2.73.

3. Systematic palaeontology

Specimen numbers are listed below in the order that they are figured.

3.1. Teeth and toothplates

Class Chondrichthyes Huxley, 1880
Subclass Euchondrocephali Lund & Grogan, 1997
Superorder Holocephali Bonaparte, 1831
Order Helodontiformes Patterson, 1965
Family Helodontidae Patterson, 1965
Genus *Helodus* Agassiz, 1838

Type species. *Helodus simplex* Agassiz, 1838. Staffordshire, England and Lanarkshire, Scotland. Moscovian.

Helodus ?simplex Agassiz, 1838
(Fig. 3a)

Material. NMS G. 2015.5.19.

Description. This tooth is high crowned, with a single central cusp. The specimen is partly embedded within matrix and around two thirds of the tooth is exposed. The central cusp is high (6.9 mm without root) and conical with tubular dentine visible over the occlusal surface. The lateral (mesial or distal) edge is straight and the occlusal surface bears a small flattened shoulder on the side of the main cusp. The lingual or labial edge is defined and undercut. The base is approximately half the height of the main cusp and, although mostly obscured by matrix, is flat along the lingual or labial surface and approximately flat along the basal edge.

https://doi.org/10.1017/S1755691018000166 Published online by Cambridge University Press

Figure 3 (a) *Helodus ?simplex* NMS G.2015.5.19. (b–k) ?Helodontidae indet.: (b) UMZC 2015.31.334 in labial (1), lingual (2), occlusal (3) and basal (4) views; (c) UMZC 2015.31.351 in labial (1), lingual (2), occlusal (3) and basal (4) views; (d) NMS G. 2015.5.28 in orolabial (1), labial (2), lateral (3) occlusal (4) and basilingual (5) views; (e) NMS G. 2015.5.28 in labial (1), lingual (2), first lateral (3), occlusal (4), basal (5) and second lateral (6) views; (f) NMS G. 2015.5.47 in labial (1), lingual (2), occlusal (3) and basal (4) views; (g) NMS G. 2015.5.17 in labial (1), lingual (2), occlusal (3) and basal (4) views; (h) NMS G. 2015.5.40 in lingual (1), labial (2), occlusal (3) and basal (4) views; (i) NMS G. 2015.5.9 in *in situ* occlusal (1), labial (2), lingual (3), occlusal (4) and basal (5) views; (j) NMS G. 2015.5.6; (k) UMZC 2015.37. Scale bars = 2 mm (a–f, h–k); 10 mm (g).

Remarks. The flat lingual or labial edge of the cusp and the flat basal edge of the base of NMS G. 2015.5.19 is similar to those of NHMUK PV P5157 from the Moscovian of Staffordshire. In contrast, the lingual and labial edges of NHMUK PV P2905 from the Moscovian of Lanarkshire are strongly arched occlusally, as is the basal margin of the base. In this way, the Whitrope Burn *Helodus simplex* is more morphologically similar to the Staffordshire teeth than to the Lanarkshire teeth. This is the earliest occurrence of *Helodus simplex*.

Helodontidae indet.
(Fig. 3b–k)

https://doi.org/10.1017/S1755691018000166 Published online by Cambridge University Press

Material. UMZC 2015.31.334 (Fig. 3b); UMZC 2015.31.351 (Fig. 3c); NMS G. 2015.5.28 (Fig. 3d); NMS G. 2015.5.28 (Fig. 3e); NMS G. 2015.5.47 (Fig. 3f); NMS G. 2015.5.17 (Fig. 3g); NMS G. 2015.5.40 (Fig. 3h); NMS G. 2015.5.9 (Fig. 3i); NMS G. 2015.5.6 (Fig. 3j); UMZC 2015.37 (Fig. 3k).

Description. These teeth have low, wide crowns with tubular dentine apparent on the surface. Cusp number ranges from one to three. The two single-cusped teeth (Fig. 3b, c) both have a crown that form a slightly curved rectangle in occlusal view with a central bulge formed by a central cusp. The overall curve of the tooth is lingually concave. The central cusp is low and inclined toward the curved lingual edge of the tooth; at this point the cusp appears triangular in lateral view. The mesial and distal ends of the tooth are slightly raised in distinct shoulders formed by a pair of much smaller, flattened cusps. The second pair of cusps incline to the lingual edge in the same way as the main cusp. The lingual wall of the main cusp is flat and perpendicular to the base. The wall is marked in one specimen by irregular and curvilinear striae that converge on the cusp apex, and in the other specimen by a smooth face with broad prominent ridge the runs parallel to the triangular occlusal edge. The base is missing in both specimens but the basal surface is flat to slightly concave.

The three-cusped form (Fig. 3g, h, j, k) has three clearly defined, high crowned cusps. The three cusps are rounded in occlusal view, triangular in lateral view and are slightly inclined at 90 degrees to the long axis of the three cusps. The middle cusp is the largest and one end cusp is slightly larger than the other. The larger end cusp is more robustly connected to the middle cusp than the smaller end cusp. In some teeth, creases can be seen running perpendicular to the long axis where the cusps join. In occlusal view, the three cusps do not form a straight line but describe a curve. The cusps incline inward toward the concavity of the curve. The labial face of each cusp curves steadily toward the cusp apex, such that in cross-section the labial face forms the hypotenuse of a right-angle triangle. In contrast, the lingual cusp surface varies from rounded and smooth to an approximately flat wall with surface ridges that radiate unevenly away from the occlusal cusp apex to the base of each cusp. The base of the tooth is preserved in one specimen and, in this example, it is approximately the height of the smallest cusp. The surface of the base shows rows of foramina along its length, about ten foramina per cusp (not all of the base is visible).

The two-cusped form (Fig. 3d, e, f) differs from the three-cusped form only in that the cusps are more rounded in occlusal view and are slightly taller relative to the cusps of the three-cusped form.

The asymmetric two-cusped form is represented by a single, large (22.5 mm long) specimen (NMS G. 2015.5.9, Fig. 3i) with evidence of in-mouth wear. The tooth is asymmetrically crescentic in occlusal view. The main cusp is situated at the wider end of the crescent and is adjoined by a smaller middle cusp and a possible third cusp or flattened tail. Micro-CT analysis shows that the base is missing and that the basal surface of the tooth is concave similar to the other, multicusped teeth. The occlusal surfaces of both cusps are flattened and the texture is pitted in comparison to the lingual and labial surfaces. This tooth is likely to have been worn through use rather than through transport.

Remarks. All of the teeth assigned to this taxon are typically helodont in the fusion of one larger middle cusp and two smaller outer (mesial and distal) cusps to form a linear composite tooth within the tooth row (Patterson 1965). They are similar in main cusp shape and overall tooth asymmetry. However, there are two obvious differences between the single- and the multi-cusped forms: The single-cusped teeth (typically 4–5 mm long) are smaller than any of the multi-cusped teeth (NMS G. 2015.5.40 is 15.4 mm long), and the two side-cusps are reduced to form two almost-flat regions. The two single-cusped teeth have different basal curvatures, UMZC 2015.31.334 is almost flat whereas UMZC 2015.31.351 is relatively strongly arched. It is likely that all forms occupied different positions within the same dental arcade, possibly in that of *Helodus simplex*.

Order Chondrenchelyiformes Patterson, 1965
Family Chondrenchelyidae Berg, 1940
Genus *Harpagofututor* Lund, 1982

Type species. *Harpagofututor volsellorhinus* Lund, 1982. Bear Gulch Member of the Heath Formation, Montana. Namurian.

Harpagofututor sp.
(Fig. 4b)

Material. NMS G. 2015.5.42

Description. Represented in Whitrope Burn by one toothplate, it is triangular in occlusal view and strongly resembles the tritoral toothplates of *Harpagofututor volsellorhinus* (Lund 1982) and, to a lesser extent, *Chondrenchelys problematica* (Finarelli & Coates 2014). The triangle shape is formed by a symphyseal edge at the hypotenuse and two slightly curved edges, one slightly longer than the other. These are the lingual and mesial edges; the orientation of the toothplate is not clear, although based on the orientation of the upper tritoral toothplates of *Harpagofututor*, the longer (11.9 mm) edge is likely to be the lingual edge, and the shorter (10.4 mm), the mesial. The toothplate has four rows of cusps which converge to a labial point. It is slightly curved, in lateral view, towards this point so that this point is angled base-wards. The individual cusps increase in height and width away from the converging point and the outermost are 2.3 mm tall. Six individual cusps are clearly visible within each cusp row and can be correlated across the four rows. Closer to the converging point, the cusp row is replaced by a ridge, possibly a seventh worn cusp.

Remarks. Micro-CT images of this tooth give new insight into the morphology of this type of tooth. Each cusp row is hollow in this rendering of the micro-CT scans, as the cavities within each cusp are joined by low density material. The labial point of the toothplate is complete with no indication of cusp addition. The symphyseal ends of two of the cusp rows are almost complete, while the other two are open indicating that addition was possible at this end. The mesial and labial edges are incomplete, revealing the low-density areas within the cusp rows. It is possible that this is a fractured surface. The truncation sites on NMS G. 2015.5.42 occur close to the cusp tips, whereas fractures are most likely to occur at the point between cusp rows where the toothplate is thinnest. Additional wear could be responsible for unusual fracture sites, however. In summary, the low-mineral content of the symphyseal, medial and lingual edges of this tooth are consistent with the assertion of Lund (1982) and Stahl (1999) that growth takes place on the symphyseal edge of the tooth, but our evidence cannot rule out the possibility that cusp row addition took place on the lingual edge, or even the mesial edge or a combination of them all. The surface of NMS G. 2015.5.42 has a partial layer of white interdenteonal tissue, similar to that noted by Lund (1982) in *Harpagofututor*.

Genus *Platyxystrodus* Hay, 1899

Type species. *Platyxystrodus striatus* Hay 1899. Armagh. Lower Carboniferous.

https://doi.org/10.1017/S1755691018000166 Published online by Cambridge University Press

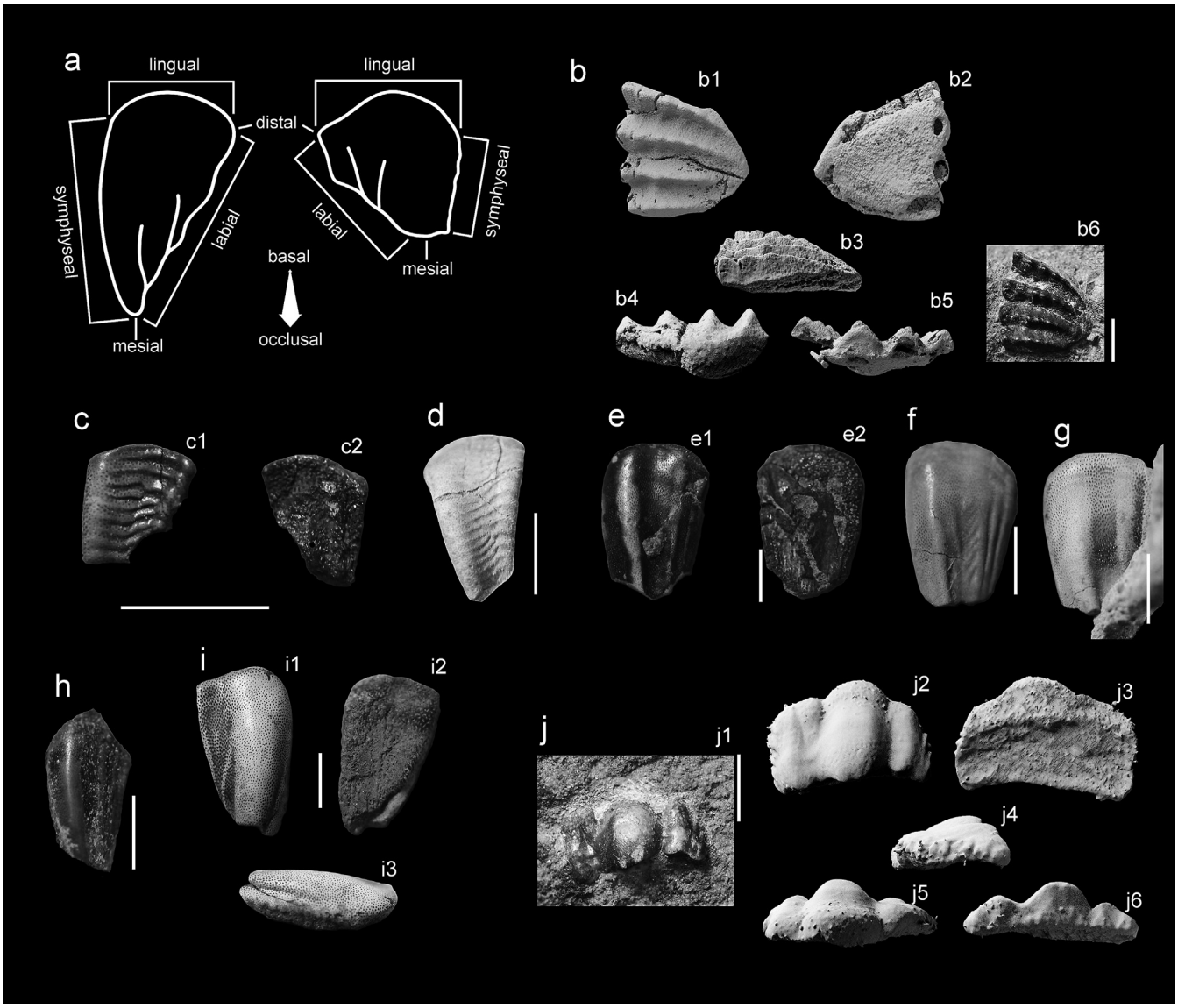

Figure 4 (a) Schematic using NMS G. 2015.5.31 and UMZC 2015.40 to demonstrate anatomical terms used to describe teeth. Based on Patterson 1992. (b) *Harpagofututor* sp., NMS G. 2015.5.42 in occlusal (1), basal (2), mesial (3), lingual (4) labial (5) and *in situ* occlusal (6) views. (c) *Platyxystrodus* sp. 1, UMZC 2015.38 in occlusal (1) and basal (2) views. (d) *Platyxystrodus* sp. 2, UMZC 2015.49. (e–h) Psephodontidae indet. 1: (e) NMS G. 2015.5.40 in occlusal (1) and basal (2) views; (f) UMZC 2015.36; (g) NMS G. 2015.5.17; (h) NMS G. 2015.5.25. (i) Psephodontidae indet. 2, UMZC 2015.32 in occlusal (1), basal (2) and symphyseal (3) views. (j) Psephodontidae indet. 3, NMS G. 2015.5.33 in *in situ* occlusal (1), occlusal (2), basal (3), lateral (4), mesial (5) and distal (6) views. Scale bars = 5 mm (a, b, d–j); 2 mm (c).

Genus diagnosis. McCoy's (1885) description of *Cochliodus striatus* is the first diagnosis of the type species, but at this time no generic diagnosis existed. Stahl's (1999) summary is as follows. Relatively small and acutely triangular toothplates. Plates are arched but not strongly enrolled mesolabially. Crown thickest along symphyseal edge where it forms a ridge on the occlusal surface. Remainder of the crown is flatter. The toothplate broadens distally, where the distal edge is sometimes raised slightly. Rows of pores mark the surface, often closely packed and parallel to each other and the lingual border.

Platyxystrodus sp. 1
(Fig. 4c)

Material. UMZC 2015.38.

Description. This tooth is rectangular in occlusal view. The lingual edge is wider than the mesial edge, giving a wide, almost triangular appearance. The width of the toothplate, together with the lack of a sharp mesial angle make this toothplate unlike *Platyxystrodus angustus* in shape. The symphyseal and labial edges are long and straight and both bear a ridge on the occlusal surface, all features typically seen in *P. striatus*. The pores of the tubular dentine form weak rows parallel to the ridges connecting the marginal ridges. The two marginal ridges are connected by a ladder-like series of ten parallel, small, but pronounced ridges which range from straight at the lingual end to more crooked at the mesial end with some ridges that fail to connect completely with the marginal ridges. These ridges are seen to a much lesser extent in *Platyxystrodus* species, particularly *P. striatus*, and tend to be distinct and have a width comparable to the pore width. The ridges on the Whitrope Burn specimen are pronounced and wave-like. The teeth are almost flat with some slight mesio-distal convexity seen from both occlusal and basal views.

Remarks. The existence of parallel dentine pores is a feature suggested by Lund (1982) to unite the Chondrenchelyiformes.

https://doi.org/10.1017/S1755691018000166 Published online by Cambridge University Press

The small size and relatively flat and rectangular shape conforms to the general form of *Platyxystrodus* toothplates described by Woodward (1889) as the upper toothplates. The ridges seen on this tooth are extremely pronounced in comparison to other *Platyxystrodus* specimens.

Platyxystrodus sp. 2
(Fig. 4d)

Material. UMZC 2015.49.

Description. This tooth is separated from *Platyxystrodus* sp. 1 on the basis of the following differences. UMZC 2015.49 is approximately twice as large as UMZC 2015.38, and is longer (9.6 mm rather than 19 mm) and narrower (6.9 mm rather than 16 mm at the widest point). The occlusal surface ridges are much less pronounced and more numerous (16 rather than ten), which may be expected as the tooth is longer.

Order Cochliodontiformes Obruchev, 1953
Family Psephodontidae Zangerl, 1981
Psephodontidae indet. 1
(Fig. 4e–h)

Material. NMS G. 2015.5.40 (Fig. 4e); UMZC 2015.36 (Fig. 4f); NMS G. 2015.5.17 (Fig. 4g); NMS G. 2015.5.25 (Fig. 4h).

Description. The crowns of these teeth are long (NMS G. 2015.5.17 is 11 mm long), low and rectangular in occlusal view. The lingual edge is symmetrically curved, with a flattened apex. In basal view the base is slightly concave in the labial-symphyseal direction but flat in the mesio-distal direction. The labial edge is straight and smooth and the symphyseal edge is slightly curved in occlusal view and smooth. The mesial edge is irregular but approximately straight in the single specimen in which this is preserved intact. The irregularity is a consequence of the ridges that truncate abruptly at the mesial end so that the edge is irregular in height. The main occlusal ridge is inset from the symphyseal edge of the tooth and runs parallel to it from the lingual edge to the mesial edge. The ridge is smooth and bluntly triangular in hypothetical cross section. Labial to the main ridge, three smaller ridges run parallel with the labial edge from the corner between the mesial and labial edges for three-quarters of the tooth length before fading away. On UMZC 2015.36 (Fig. 4f), mesially-directed superficial ridges come off the most mesial of these three ridges and fill half of the sulcus created between the main ridge and the smaller ridges.

Remarks. Large rectangular crowns with ridges place these teeth within the Cochliodontiformes. Flat to slightly concave bases support inclusion within Psephodontidae rather than Cochliodontidae.

Psephodontidae indet. 2
(Fig. 4i)

Material. UMZC 2015.32.

Description. This tooth is long (15.2 mm) and approximately rectangular. The lingual edge is rounded and asymmetrical and both mesial and distal edges are convex. The main occlusal ridge is wide, high and domed and takes up around three-fifths of the tooth width at its widest point. The ridge runs down the symphyseal side of the toothplate from the lingual edge and narrows mesially to the mesial edge. The occlusal surface labial to the main ridge is slightly concave and the tooth thins considerably. The lingual edge meets the labial edge at almost a right angle to form a clear distal wing. At the lingual end, the occlusal ridge forms the symphyseal edge of the tooth, but mesially the ridge is inset with a sulcus at its base. Basal to this sulcus the edge is crenulated, indicating that a pair of these teeth probably abutted another symphyseal tooth that tessellated with the curved symphyseal edge. The mesial point is partially fractured in the only representative specimen of this tooth, but is likely to have been convex to straight in occlusal view. Part of the base is attached in this specimen but has been well worn. It is clear that the basal surface of the crown is concave in the mesio-distal direction, but only slightly concave in the linguo-labial direction.

Remarks. A large rectangular crown with a crushing crown places this tooth within the Cochliodontiformes. A slightly concave base supports inclusion within Psephodontidae rather than Cochliodontidae.

Psephodontidae indet. 3
(Fig. 4j)

Material. NMS G. 2015.5.33.

Description. This tooth is represented by a single micro-CT scanned specimen. The occlusal surface visible out of the matrix (Fig. 4j6) indicates that this tooth is well worn in life and also probably abraded in the matrix as it was exposed to fluvially entrained clasts and sediment. The tooth is semicircular in occlusal view and composed of three main asymmetric lobes separated by shallow indentations on the curved long edge, here assumed to be the lingual edge. All lobes thin lingually and laterally to meet the curved lingual edge, are thickest in the middle of the lobe but thin only slightly to the opposite, here assumed the labial, edge where they meet a labial face perpendicular to the base. The lingual edge bears marginal ornament similar to the crenulations seen around the toothplate, but in which the sloping edges bear ridges that bifurcate basally and become more pronounced. The middle lobe is longest, widest and is the most strongly convex. It is slightly asymmetrical and is inclined to one side, the lateral lobes fit around this inclined lobe so that they form opposing wedge-shapes, the smallest lobe narrows lingually and the medium lobe narrows labially. The lateral lobes are weakly divided into two sub-lobes at their widest end. The main lobe shows a thinning in a curve parallel with the lingual edge, suggestive of a growth line. However, this is not shared with the lateral lobes, which are thick and even along their length. If this is a growth line, then the implication is that the main lobe was formed and accreted lingually before additional lobes were added laterally. The base consists of two concavities separated by a ridge. The ridge corresponds roughly to the possible growth line on the occlusal surface of the main lobe, but the ridge extends across the base of all lobes. The concavity on the lingual side of the ridge is narrow and is at a slight angle to the main base, so that the lingual edge of the tooth is slightly upraised.

Remarks. Growth lines across the main lobe of the tooth are not shared by the lateral lobes, suggesting that this tooth was accreted from different directions throughout life, or that lobes were accreted at different times of life.

Order Cochliodontiformes Obruchev, 1953 *incertae sedis*
Whitropus gen. nov.

Derivation of name. The name *Whitropus* reflects the type and only locality at which this taxon occurs. The masculine ending –us is chosen.

Type species. *Whitropus longicalcus* gen. et sp. nov.

https://doi.org/10.1017/S1755691018000166 Published online by Cambridge University Press

Genus diagnosis. Cochliodont-like toothplate, slightly enrolled to flat. Symmetrically triangular to asymmetrically polygonal. Ridges on the occlusal surface of the tooth form predictable patterns depending on tooth type, but all consist of a main occlusal ridge, offset from the middle of the long axis, extending the length of the tooth, with anastomosing ridges pointing towards the narrowest end of the tooth, and up to three smaller occlusal ridges extending the length of the tooth on the opposite side of the long axis.

Whitropus longicalcus gen. et sp. nov.
(Fig. 5a–i)

Derivation of name. *longicalcus* is composed of the Latin for longitudinal (longitudo) and spur (calcar) which describes the longitudinal occlusal ridges with anastomosing spur-like projecting ridges.

Holotype. NMS G. 2015.5.31, Tournaisian, Lower Carboniferous, Ballagan Formation. Whitrope Burn, Scotland, UK.

Figured specimens. NMS G. 2015.5.31 (Fig. 5a); NMS G. 2015.5.26 (Fig. 5b) NMS G. 2015.5.30 (Fig. 5c); NMS G. 2015.5.25 (Fig. 5d); NMS G. 2015.5.25 (Fig. 5e); NMS G. 2015.5.3 (Fig. 5f); NMS G. 2015.5.30 (Fig. 5g); UMZC 2015.39 (Fig. 5h); UMZC 2015.40 (Fig. 5i).

Diagnosis. As for genus.

Description. There are two morphotypes within this taxon, Type I and II. See Figure 4a for explanation of anatomical terms.

Type I is represented by NMS G. 2015.5.31, NMS G. 2015.5.26 and NMS G. 2015.5.30 (Fig. 5a–c). These toothplates have a low triangular crown in occlusal view, NMS G. 2015.5.31 (Fig. 5a), for example, is 17.5 mm long and the crown is approximately 2.7 mm tall. The lingual edge is convex, as is the long and smooth symphyseal edge. The labial edge is straight, slightly convex or slightly concave and changes at the midpoint from a smooth edge lingually to a more irregularly wave-like edge towards the mesial angle. This angle also marks the point where the mesial portion of the tooth rises to meet the main occlusal ridge. This rise in the mesial portion of the tooth is a factor of the occlusal convexity seen across the tooth. The convexity varies amongst these specimens from an almost flat toothplate (NMS G. 2015.5.31; Fig. 5a) to the moderately convex toothplates (NMS G. 2015.5.26, NMS G. 2015.5.30; Fig. 5b, c). The main occlusal ridge is relatively wide, occupying around one third of the width of the tooth. It extends from the mesial angle, down the symphyseal edge to the symphyseal end of the curved lingual edge. The ridge is not clearly inset from the edge of the tooth, instead together they share a symphyseal edge. More worn ridges extend mesially from the main ridge. The occlusal surface labial to the main ridge is marked with three to four thin, parallel ridges running from just short of the lingual edge to points along the mesial part of the labial edge. There is a small distal wing which continues the convex shape which runs diagonally across the tooth and results in the labial edge being slightly depressed relative to the rest of the occlusal surface.

Type II is represented by NMS G. 2015.5, NMS G. 2015.5.25, NMS G. 2015.5.3, NMS G. 2015.5.30, UMZC 2015.39 and UMZC 2015.40. (Fig. 5d–i). These toothplates are broad and polygonal in occlusal view, UMZC 2015.40 (Fig. 5i), for example, is 10.5 mm long and the cusp is approximately 4 mm tall. They possess four edges with a curved fifth edge forming the lingual edge. They range from slightly (Fig. 5e) to highly (Fig. 5i) asymmetric, the two lateral edges are unequal in length, the labial is around twice the length of the symphyseal and the curved lingual edge leans slightly toward the longer lateral edge. There is one short mesial edge. The labial edge has an angle in the middle so that there appear to be two labial edges, one more lingual and one more mesial. The labial edges range in length and concavity. The occlusal surface is convex and show similar patterns of ridges revealed by differential wear patterns in the tubular dentine. The main occlusal ridge runs from the junction between the labial and mesial edges to the apex of the lingual edge convexity. Short and narrow ridges run mesially off both sides of this main ridge at regular intervals; the total number is four to five on each side, depending on the length of the tooth. Two to three narrower ridges parallel to the main ridge occupy the surface between the main ridge and the short or concave lateral side. In some teeth (Fig. 5a, g, for example) a wide but short triangular ridge is also inserted between the main ridge and the long lateral edge on the lingual side. The long and unbroken lateral edge bears crenulations formed by regular projections along the tooth edge (Fig. 5d2, e2). Both tooth types have concave basal surfaces with evidence of growth lines.

Remarks. Specimen NMS G. 2015.5.26 is more worn than NMS G. 2015.5.31 and shows several differences that are likely to be a consequence of growth. Wear has obscured most of the ridges on the occlusal surface, but the fine lines that remain corroborate those seen in the less-worn specimen. Growth lines on the lingual edge show that recent accretion has shifted the apex position of the curve lingually, away from the occlusal ridge. NMS G. 2015.5.26 is wider in relation to length and the midpoint on the labial edge is also marked by a slight change in angle in this specimen. This makes the mesial angle of the tooth slightly less acute than NMS G. 2015.5.31. The occlusal surface of the tooth is weakly curved. None of these specimens may be seen in basal views. Wide crushing crowns place these teeth within the Cochliodontiformes. Acutely triangular tooth plate shape and concave bases support inclusion within Cochliodontidae rather than Psephodontidae, but the bases of type I teeth are not strongly convex, and so we cannot rule out inclusion within Psephodontidae. The degree of enrolling in type I teeth and the triangular shape is comparable to flatter cochliodont teeth such as *Sandalodus*, and some *Deltodus* teeth. Type II teeth have a slightly more pronounced curvature.

The Whitrope Burn teeth have complex, regular and longitudinally organised surface detail which sets them apart from other Cochliodontidae which tend to be smooth or, like *Deltodus sublaevis, D. grandis* and *D, grandis*, have ridges running across the tooth parallel with the lingual edge. The surface detail is unique within Palaeozoic holocephalans and so conserved within these tooth types that we consider it useful for these teeth to be assigned to a new genus. Type II toothplates are concave and it is likely that these form part of the enrolled mandibular dentition within the mouth, while Type I may form the flatter palatal dentition (see Figure 5i2 for one possible reconstruction of how these teeth may have fitted together in life). The symphyseal margins of all lower, mandibular teeth are crenulated, as commonly seen in *Psephodus* toothplates and support the reconstruction of a mandibular dentition with tessellated toothplates rather than the tightly enrolled dentition typical of cochliodonts such as *Cochliodus*.

Family Cochliodontidae Owen 1867
Genus *Deltodus* Morris & Roberts, 1862
(*ex*. Agassiz MS 1859 (unpublished))

Type species. *Poecilodus sublaevis* Agassiz, 1838. Lower Carboniferous Armagh Group, Northern Ireland. Viséan.

https://doi.org/10.1017/S1755691018000166 Published online by Cambridge University Press

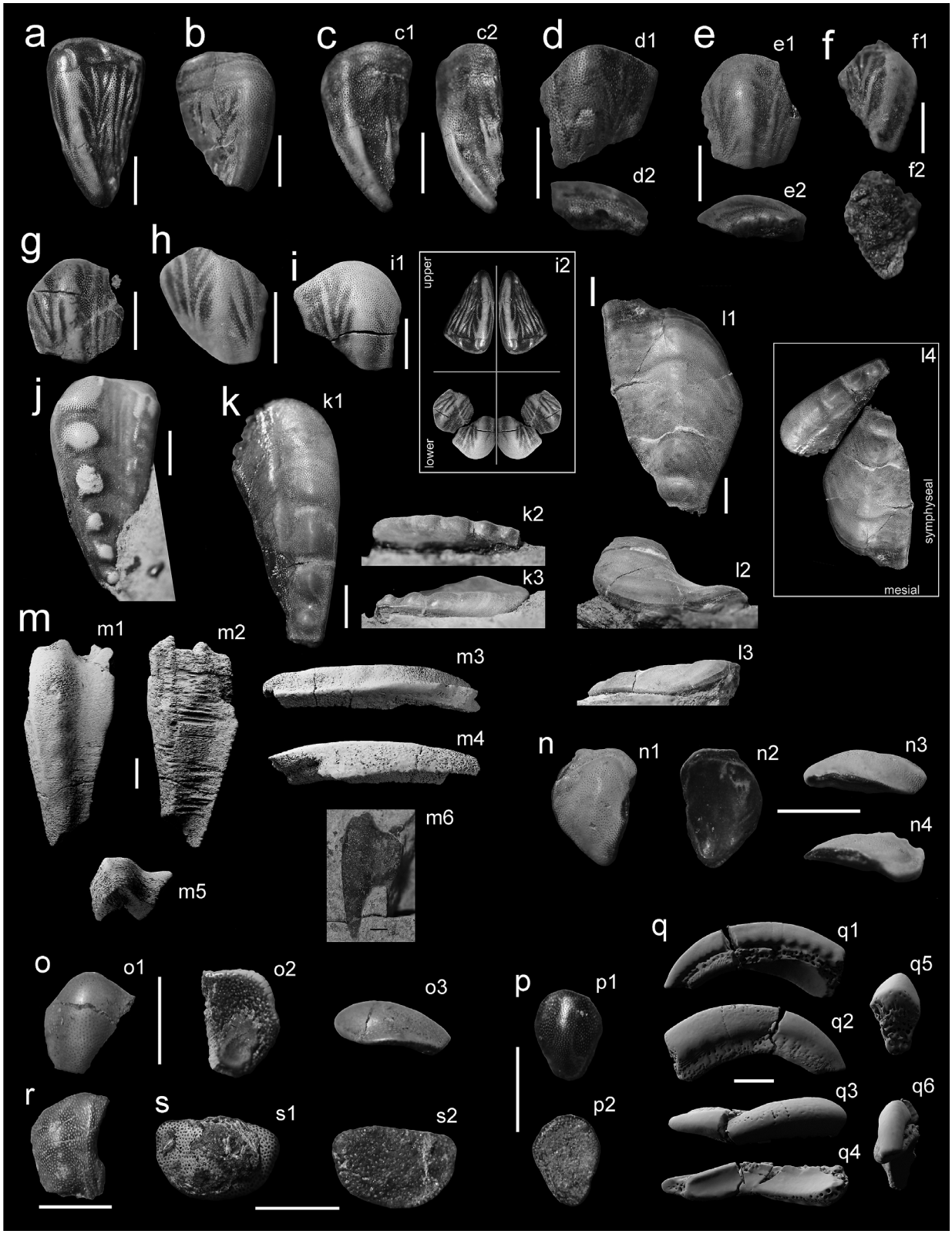

Figure 5 (a–i) *Whitropus longicalcus* gen. sp. nov.: (a) NMS G. 2015.5.31; (b) NMS G. 2015.5.26; (c) NMS G. 2015.5.30 in occlusal (1) and labial (2) views; (d) NMS G. 2015.5.25 in occlusal (1) and lateral (2) views; (e) NMS G. 2015.5.25 in occlusal (1) and lateral (2) views; (f) NMS G. 2015.5.3; (g) NMS G. 2015.5.30; (h) UMZC 2015.39; (i) UMZC 2015.40 in occlusal view (1) and one possible reconstruction of the dentition (2). (j–m) *Deltodus tubineus* sp.nov.: (j) NMS G. 2015.5.1; (k) NMS G. 2015.5.2 in occlusal (1), distal (2) and mesial (3) views; (l) UMZC 2015.48 in occlusal (1), lingual (2) and mesial (3) views, and reconstructed in position with NMS G. 2015.5.2, relative tooth sizes have been changed (4); (m) NMS G. 2015.5.53 in occlusal (1), basal (2), mesial (3), symphyseal (4), labial (5) and *in situ* occlusal (6) views. (n–o) *Deltodus* sp.: (n) UMZC 2015.33 in occlusal (1), basal (2), mesial (3) and distal (4) views; (o) UMZC 2015.31.332 in occlusal (1), basal (2) and distal (3) views. (p) Cochliodontiformes indet. 1., UMZC 2015.31.320 in occlusal (1) and basal (2) views. (q) Holocephali indet. 1, UMZC 2015.52 in lateral (1, 2), occlusal (3), basal (4), distal (5) and mesial (6) views. (r) Holocephali indet. 2, NMS G. 2015.5.5. (s) Holocephali indet. 3, UMZC 2015.31.331 in occlusal (1) and basal (2) views. Scale bars = 5 mm.

https://doi.org/10.1017/S1755691018000166 Published online by Cambridge University Press

Genus diagnosis. Diagnosed by McCoy (1855). Terminal tooth obliquely trigonal and slightly convoluted, median tooth narrow and much convoluted. All teeth longitudinally marked with thick step-like, oblique, flattened wrinkles, apparently at right angles to the articular edges. Porous surface.

Deltodus tubineus sp. nov.
(Fig. 5j–m)

Derivation of name. 'Tubineus' being the Latin translation of cone. This name is chosen to reflect the prominent cone-shaped teeth on the symphyseal ridge of the tooth.

Holotype. NMS G. 2015.5.2. Tournaisian, Lower Carboniferous, Ballagan Formation. Whitrope Burn, Scotland, UK.

Figured specimens. NMS G. 2015.5.53 (Fig. 5m); NMS G. 2015.5.1 (Fig. 5j); NMS G. 2015.5.2 (Fig. 5k); UMZC 2015.48 (Fig. 5l).

Diagnosis. As for genus, but with four to six pronounced conical cusps arranged linearly along the symphyseal occlusal ridge. No narrow shelf symphyseal to the occlusal ridge.

Description. The new species is represented by two tooth types with very similar morphology. The first morphotype (Fig. 5j, k) is represented by a long, curved triangle in occlusal view. NMS G. 2015.5.53 (Fig. 5m), for example, is 23.5 mm long and 11.6 mm wide. A series of six bluntly domed cusps extends down the convex symphyseal side of the toothplate, the size increases towards the broad, lingual end of the toothplate. The cusps become wider but shallow and less distinct lingually. These cusps are similar in appearance to those radiating across the surfaces of the posterior toothplates of *Chondrenchelys* and *Harpagofututor*. The concave, labial, side of the toothplate is slightly raised in a ridge which varies from sharp to domed, depending on whether the highest cross-section point is on the edge of the toothplate or inset from the edge. Tubular dentine is clear on worn and unworn surfaces.

A second morphotype (Fig. 5l) is included within this taxon. It is similar to the first morphotype of *Deltodus tubineus* but different in a number of details. The toothplate is wider in occlusal view (17.8 mm wide and 29.5 mm long), and the sides are nearly straight so that the toothplate lacks the curve of morphotype one. The same relationship exists in the junction between the short and the long sides. Four bluntly domed cusps with wider bases than seen in morphotype are ranged down the symphyseal side. The ridge opposite the cusps is domed. This toothplate is more curved across the lingual edge of the tooth than morphotype one so that the rounded junction between the long and short sides curves towards the base, as does the diametrically opposite ridge close to the mesial point of the triangular toothplate.

Remarks. The following features identify this taxon as *Deltodus*: toothplate large and triangular, curved labio-mesially, undulating along length of prominent symphyseal ridge, slightly raised distal wing. This is probably the upper, palatine plate. Two articulated toothplates of *Deltodus sublaevis* (NHMUK PV P2441) show large and small teeth next to each other, with the larger plate mesial to the smaller plate (Davis 1883, pl. LII, fig. 9). We suggest that this is the relationship that the two morphotypes of *Deltodus tubineus* have, with the first morphotype occurring distal to the larger toothplate, possibly as reconstructed in Figure 5l4. The Whitrope Burn *Deltodus* has striking similarities with *D. sublaevis*, the main differences being the lack in *D. sublaevis* of the pronounced occlusal cusps seen in the Whitrope Burn specimens, and the lack in the Whitrope Burn specimens of a narrow symphyseal shelf. Specimen UMZC 2015.48 seems, in occlusal view, to carry a very small symphyseal shelf. However, the mesial view shows that this is a decrease in slope angle rather than an extended and flattened shelf as seen in *D. sublaevis*.

Deltodus sp.
(Fig. 5n–o)

Material. UMZC 2015.33, UMZC 2015.31.332.

Description. The teeth representing the third species attributed here to *Deltodus* show a small morphological difference that is likely to be due to intraspecific variation; this is made clear in the following description. The tooth is teardrop-shaped or semi tear-dropped in occlusal view. The occlusal surface is mainly domed but flattens toward the symphyseal and, to a lesser extent, labial edges. The symphyseal and labial edges are smooth with no ornament and lift slightly toward the occlusal surface. This concavity of the symphyseal and labial edges is more pronounced in specimen UMZC 2015.33 (Fig. 5n). The lingual edge in both teeth is curved. The main difference between the teeth is that the labial and symphyseal edges of UMZC 2015.31.332 (Fig. 5o) are separated by a clear angle, whereas in UMZC 2015.33 (Fig. 5n) this angle is much less pronounced and the edge is convexly curved. In this way, UMZC 2015.33 appears teardrop-shaped, whereas UMZC 2015.31.332 appears wedge-shaped. This tooth is not strongly enrolled but is concave.

Remarks. Only two complete specimens of this tooth type were found in the sample. Further sampling is necessary to show whether these are two distinct morphologies or joined by a gradient of tooth shapes, suggestive of intraspecific variation.

Cochliodontiformes indet. 1.
(Fig. 5p)

Material. UMZC 2015.31.320.

Description. This tooth is represented by a single specimen. It is pear-shaped in occlusal view and the surface slopes gently down to the base at the edges. The central portion of the occlusal surface is strongly convex as a domed ridge extends down the long axis. Two concave semi-circular fields sit on either side of the ridge at the widest part of the tooth.

Remarks. This tooth shows some similarities to the *Helodus rankinei* (Stahl 1999) in the centrally domed shape, but lacks any indication of marginal crenulations associated with tooth row fusion.

Holocephali indet. 1
(Fig. 5q)

Material. UMZC 2015.52.

Description. This tooth is represented by a single whole specimen. Fragments of similar teeth are common in the Whitrope Burn sediments and it is likely that they represent a taxon that forms a significant part of the chondrichthyan fauna. This tooth has a deep base with a flat crown bearing tubular dentine. No teeth of this type exist without the base and it is possible that, due to their length and thinness, the crowns alone have a low preservation potential. The crown is approximately 22.8 mm long, curved and smooth when reconstructed through micro-CT scans. In cross-section, the crown forms a low blunt triangle. Both long edges have crenulations similar to those documented in other teeth although the crenulations on one side are much more pronounced. Apart from the difference in crenulation size, the crown is symmetrical about the long axis. The base is deeply concave in both axes and is asymmetrical about the long axis. The base is

https://doi.org/10.1017/S1755691018000166 Published online by Cambridge University Press

deeper on one long edge than the other, on the side of the less pronounced crenulations. The base twists mesially to the side with the more pronounced crenulations.

Holocephali indet. 2
(Fig. 5r)

Material. NMS G. 2015.5.5.

Description. This tooth is represented by a single specimen. It is approximately rectangular in basal view and longer in, what we interpret as, the labio-mesial direction. Almost the entire length of one lateral edge is concave, interpreted as labial. A thin but acute ridge is inset from the labial edge and runs parallel to it from the mesial corner (the lower right hand corner, as orientated in Figure 5r) of the tooth, almost to the end of the mesial edge. A short second ridge originates from the same corner and lies inside the main ridge, closer to the midline of the tooth. The symphyseal and lingual edges are curved. A second ridge runs parallel to the first, acute ridge. This second ridge is less acute and in cross-section is more broadly domed than the first. Little differential wear is observed on this tooth. The tooth has an overall 'lumpy' and irregular appearance in contrast to many of the other teeth which tend to be smooth and uniform in texture.

Remarks. The taxonomic placement of this form is uncertain. It is holocephalan but not chondrenchelyiform due to the lack of orthotrabeculine pore organisation.

Holocephali indet. 3
(Fig. 5s)

Material. UMZC 2015.31.331.

Description. The tooth is semi-circular in occlusal view and is 7.2 mm across the longest edge. The occlusal surface is convex, with an apparently even wear distribution over the tubular dentine, although some parts of the surface are obscured by hard-to-remove matrix. Each edge slopes gently down to the contact with the basal surface. As in many of the teeth described above, it is likely that most of the base is missing. The basal surface preserved in this case is gently concave.

Subclass Elasmobranchii Bonaparte, 1838
Order Ctenacanthiformes Glikman, 1964
Family Ctenacanthidae Dean, 1909
Genus *Cladodus* Agassiz, 1843

Type species. *Cladodus mirabilis* Agassiz, 1843. Lower Carboniferous Armagh Group. Northern Ireland. Viséan.

Cladodus ?sp.
(Fig. 6a–c)

Material. UMCZ 2015.50 (Fig. 6a); UMCZ 2015.51 (Fig. 6b); tentatively NMS G. 2015.5.30 (Fig. 6c).

Description. This tooth has a large main cusp and two pairs of accessory cusps. The main cusp is recurved, linguolabially compressed and sigmoid in lateral view. The convex cusp base carries a triangular indentation. The tooth exposed by mechanical and chemical preparation (NMS G. 2015.5.30; Fig. 6c) shows several large and parallel striations running up the length of the main cusp. Ornament is not visible on the micro-CT scanned teeth because the resolution of the scans is not sufficient to reveal these fine details. The main cusp of one specimen (UMZC 2015.50; Fig. 6a) leans slightly toward, or possibly away from, the symphyseal edge. The accessory cusps of all teeth are worn and fractured and consequently it is difficult to tell which, if any, were larger. UMZC 2015.51 (Fig. 6b) possesses two accessory cusp pairs, the cross sections of which suggest that the distal pair were slightly larger than the proximal pair. UMZC 2015.50 (Fig. 6a) possesses three accessory cusps on the side to which the main cusp leans, and two on the other side. The cusps in the group of three are of dissimilar sizes – the middle cusp is larger in cross-section than those either side of it. The middle cusp was likely to be taller than them, but of a similar size to those in the cusp pair on the other side of the main cusp, so that this side would have looked similar to the other, but with an additional small accessory cusp added distally.

The base is flattened and forms a rounded trapezoid in basal view. The occlusal side of the base has an uneven basolabial shelf running along its length between the proximal accessory cusp pair. There is a pronounced incision along the labial edge (in labial view) between the bottom of the cusps and the base. This incision lies parallel to a ridge that forms the labial edge of the base in basal view. The base is shallowly concave with a strong ridge inset from, and parallel to, the labial edge.

Remarks. NMS G. 2015.5.30 is tentatively assigned to this taxon, as the accessory cusplets and detail on the base is missing due to taphonomic wear. The labiolingual compression and labial depression of the main cusp is similar to that seen in UMCZ 2015.50 and UMCZ 2015.51, as is the proportion of the main cusp to the base in labial view.

These teeth are similar to those of *Cladodus elegans* and *Cladodus mirabilis*, found in the Viséan of Scotland (Newberry & Worthen 1870; Duffin & Ginter 2006) and Northern Ireland (Agassiz 1843; Duffin & Ginter 2006), respectively. The proportions of the multi-cusped morphology are consistent with that of *Cladodus*, as is the presence of orolingual and basolabial ridges. There are few differences between *C. elegans* and *C. mirabilis;* the accessory cusps are shorter and narrower in *C. elegans*, the main cusp carries a crista and on the labial face of the cusp the striae are more regular and are arranged parallel to the cristae (Ginter *et al*. 2010). The outer cusps also seem to be slightly more inclined away from the midline in the few specimens of *C. elegans* than those of *C. mirabilis*. We suggest that the Whitrope Burn *Cladodus* is more similar to *C. elegans* than *C. mirabilis*. NMS G. 2015.5.30 displays regular striae. The main cusp of UMZC 2015.50, in particular, displays an edge which may represent a crista. No complete outer cusps exist in the Whitrope Burn specimens; however, the fragmented stumps that remain on UMZC 2015.50 are inclined outwards at an exaggerated angle. However, as the morphology of the Whitrope Burn specimens is only inferred from micro-CT scans and the conspecific nature of NMS G. 2015.5.30 is tentative, we prefer to leave them unassigned at species level. Further specimens may resolve which of the *Cladodus* species this tooth has stronger affinities with. The specimens from Whitrope Burn measure approximately 4 mm across the base and are much smaller than *Cladodus* seen in the Avon Gorge, where some *Cladodus* specimens (e.g., BRSUG 1361, BRSUG 11477) reach approximately 3 cm or 4 cm across the base.

Cohort Euselachii Hay, 1902
Superfamily Protacrodontoidea Zangerl, 1981
Family Protacrodontidae Cappetta, Duffin & Zidek, 1993
Genus *Protacrodus* Jaekel, 1925

Type species. *Protacrodus vetustus* Jaekel, 1925. Bad Wildungen, Germany. Frasnian.

Protacrodus sp.
(Fig. 6d)

https://doi.org/10.1017/S1755691018000166 Published online by Cambridge University Press

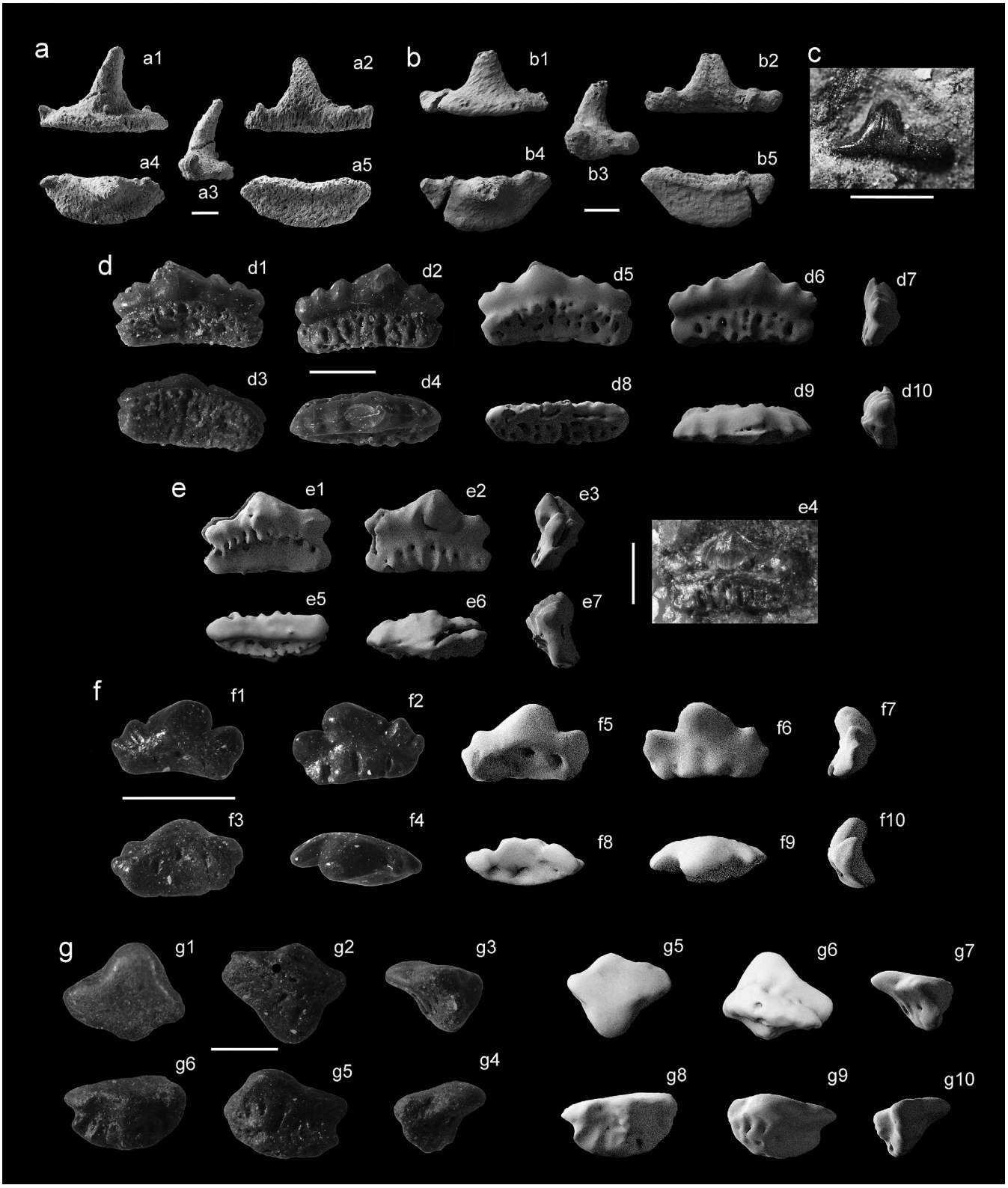

Figure 6 (a–c) *Cladodus* ?sp.: (a) UMCZ 2015.50 in lingual (1), labial (2), lateral (3), occlusal (4) and basal (5) views; (b) UMCZ 2015.51 in lingual (1), labial (2), lateral (3), occlusal (4) and basal (5) views; (c) NMS G. 2015.5.30 in labial view. (d) *Protacrodus* sp., photographs of UMZC 2015.41 in labial (1), lingual (2), basal (3) and occlusal (4) views, and μ-CT scan models in labial (5), lingual (6), first lateral (7), basal (8), occlusal (9) and second lateral (10) views. (e) *Deihim* sp., UMZC 2015.42 in labial (1), lingual (2), first lateral (3), *in situ* lingual (4) basal (5), occlusal (6) and second lateral (7) views. (f) Protacrodontidae indet., photographs of UMZC 2015.43 in labial (1), lingual (2), basal (3) and oral (4) views, and μ-CT scan models in labial (5), lingual (6), first lateral (7), basal (8), occlusal (9) and second lateral (10) views. (g) *Cooleyella* sp., photographs of UMZC 2015.35 in occlusal (1), basal (2), first lateral (3), labial (4), lingual (5) and second lateral (6) views, and μ-CT scan models in occlusal (5), basal (6), first lateral (7), labial (8), lingual (9) and second lateral (10) views. Scale bars = 1 mm.

https://doi.org/10.1017/S1755691018000166 Published online by Cambridge University Press

Material. UMZC 2015.41.

Description. This tooth is 2.2 mm long and high-crowned with one main cusp inclined towards the presumed medial side of the row of cusps. Three accessory cusps are present on the presumed distal side of the cusp row, and two accessory cusps are present on the short side. All cusps are covered by a continuous cap of enameloid and are joined by a pronounced crista which runs the length of the tooth. Additionally, both lingual and labial faces of each cusp have a single crista-like ridge running from the tip to halfway down the cusp. In occlusal view, the cusps form a slightly curved ridge, the apex of which is on the labial side. The crown is slightly constricted where it meets the base. The base is similar in height to the crown from the labial aspect but is much shorter – less than half – on the lingual aspect. Consequently, the base is much thinner on the lingual aspect and can be seen to be slightly concave in basal view. Seven large nutrient grooves are present on the labial side of the base, alongside approximately six foramina concentrated around the base-cusp junction. Approximately 11 foramina are present on the lingual side of the base; one of these is larger than the rest and lies directly below the main cusp, but no large grooves are found here. This vascularisation is anaulacorhize.

Remarks. Unlike most *Protacrodus* species, the accessory cusps decrease in size away from the main cusp, rather than the middle cusp being largest. This, along with the similarity between all other features described above, unites this tooth with AU12529 described and figured by Behan *et al*. (2012, fig. 5A–D). This tooth is only represented by a single specimen and so it is left in open nomenclature.

Genus *Deihim* Ginter, Hairapetian & Klug, 2002

Type species. *Deihim mansureae* Ginter, Hairapetian & Klug, 2002). Hutk, Kerman Province, Iran. Famennian.

Deihim sp.
(Fig. 6e)

Material. UMZC 2015.42.

Description. This taxon is represented by a single tooth. The lingual aspect of the tooth is exposed and beautifully preserved, but the labial face is buried in matrix and its description is based on micro-CT scan data. This tooth measures 1.2 mm in height from the lingual aspect. The tooth is high crowned, with a triangular main cusp flanked by a single pair of square accessory cusps. The main cusp is almost twice the height of the accessory cusps and all three cusps are joined by a strong crista. The square shape of the accessory cusps is formed by a prominence on the outermost edges of the cusps, much like a second cusp tip. All cusps are slightly lingually inclined, so that the crista is lingually offset, the labial face of the crown is bulbous and the lingual face is flatter. The lingual face of the main cusp bears three distinct, straight ridges radiating base-wards from the cusp tip. The central ridge is vertical and extends approximately halfway down the main cusp. The two outer ridges form an angle of 43° with the middle ridge and extend approximately three-quarters of the length of the main cusp. Each accessory cusp has one ridge. This starts on the side of the cusp apex and extends at an angle of 43° with the occlusal–basal plane. The accessory cusps have one ridge that starts on the main-cusp side of the accessory cusp tip and travels towards the main cusp in a near-symmetrical relationship to the long radiating ridges of the main cusp. This accessory cusp ridge lies parallel to a second ridge on the outer edge of the accessory cusp. The unusual square shape of the accessory cusps, if more distinct, would separate each cusp pair to look like two cusp pairs with separate cusp tips and a single ridge on each. The labial face of the crown is sharply convex, particularly on the main cusp, and carries eight small and separate projections at its base. The crown is constricted towards the junction with the base, and on the labial side, the constriction is sharp and slightly arched along its length. The base is rectangular and is the same length as the crown at the extent of the outer cusp tips. It is linguo-labially compressed and approximately three quarters of the height of the main cusp. The base is inclined labially by approximately 30°. Seven vertical grooves on the labial face of the base terminate in foramina. Seven large foramina also puncture the occlusal edge of the base on the lingual aspect.

Remarks. This tooth closely resembles the posterior teeth of *Deihim mansureae* (Ginter *et al*. 2002) in crown shape, particularly the presence of a lingually inclined crown, square shaped accessory cusps, labial projections and strongly ridged and radiating ornament. However, the ridges on UMZC 2015.42 are much straighter than on the Armenian *Deihim* specimens (Ginter *et al*. 2010) and the cusp outlines are more acutely triangular than the low and rounded triangles of the posterior teeth from Armenia or Iran. The base of UMZC 2015.42 is similar in shape to the rectangular bases of the Iranian examples of *Deihim mansureae.* UMZC 2015.42 is larger than recorded specimens of *Deihim mansureae*. We suggest that this is a posterior tooth of a larger UK *Deihim* species, which will remain in open nomenclature as only one example of this tooth is complete and identifiable.

Protacrodontidae indet.
(Fig. 6f)

Material. UMZC 2015.34.

Description. This tooth shows some wear and the following description indicates which features have likely been affected by this. The tooth is 1.2 mm long and high-crowned, with one main cusp inclined to one side and towards the lingual aspect. Two accessory cusps are present on the side away from the inclination of the main cusp, and one accessory cusp is present on the mesial side which the main cusp inclines towards. The latter, single accessory cusp is the largest of the accessory cusps with a width over half that of the main cusp. The remaining two cusps decrease in size away from the main cusp and are, together, approximately equal to the width of the largest accessory cusp. The cusps are joined by a crista visible on the main cusp and the second largest cusp, but are not seen on the two smallest accessory cusps, possibly due to wear. Two parallel ridges are seen to run down the labial surfaces of the cusps from the tips to the cusp-base junction. These are relatively wide ridges, with no acute angle of surface disruption; this may be original morphology, or sharp ridges may have been worn down by transport. The lingual aspect of the cusps is similarly ornamented with parallel ridges; in this aspect, however, the number per cusp is not consistent and varies from one to two. The acuteness of the ridge also ranges from subtle in the largest accessory cusp to sharp in the second largest accessory cusp. The crown meets the base at an angle with almost no constriction. The base is taller, by around 25 %, than the crown from the labial aspect but is much shorter – just over half – on the lingual aspect. The main cusp seems to have undergone wear in the occlusal view possibly as a result of in-life use, as well as the taphonomic wear evident on the rest of the tooth. This may mean that the depth of the base relative to the crown has been overestimated. The base is much thinner on the lingual aspect and

https://doi.org/10.1017/S1755691018000166 Published online by Cambridge University Press

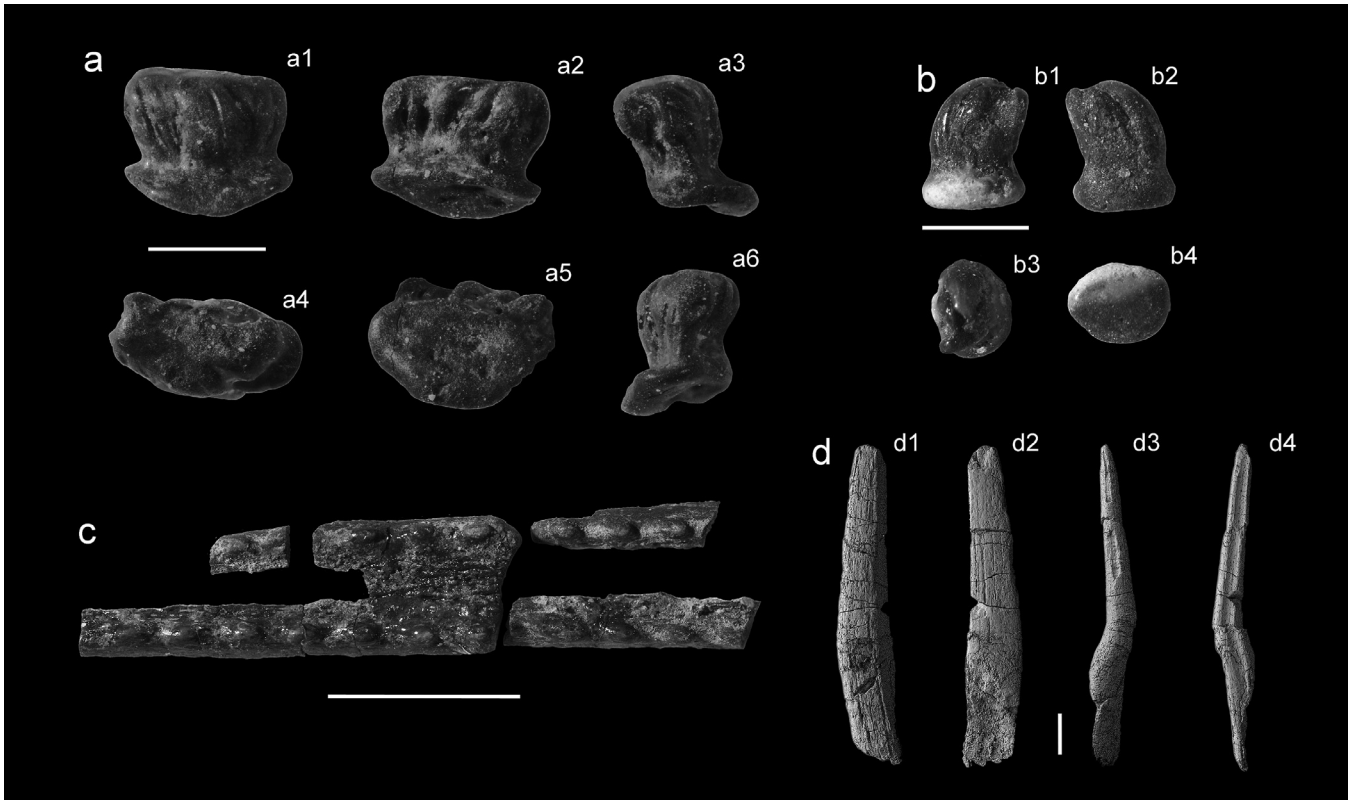

Figure 7 (a–b) Ctenacanth-type dermal denticles: (a) UMZC 2015.44 in first lateral (1), second lateral (2), third lateral (3), crown (4), base (5) and fourth lateral (6) views; (b) UMZC 2015.45 in first lateral (1), second lateral (2), crown (3) and basal (4) views. (c–d) Hybodontiformes fin spines: (c) UMZC 2015.46; (d) UMZC 2015.47 in left lateral (1), right lateral (2), mesial (3) and posterior (4) views. Scale bars = 1 mm (a, b); 5 mm (c); 2 cm (d).

can be seen to be deeply concave in basal view. Two large nutrient grooves and two large foramina are visible on the lingual aspect of the tooth, each evenly spaced on a third of the base. Approximately five very small foramina are visible on the lingual side of the base. One large foramen is placed on the labial edge of the basal surface of the base, directly below the main cusp.

Remarks. This tooth is very similar to the *Protacrodus* sp. tooth described above, except for the number of cusps and basal foramina.

Subcohort Neoselachii Compagno, 1977
Family Anachronistidae Duffin & Ward, 1983
Genus *Cooleyella* Gunnell, 1933

Type species. *Cooleyella peculiaris* Gunnell, 1933, Cherryvale Shale, Kansas City, Missouri. Pennsylvanian.

Cooleyella sp.
(Fig. 6g)

Material. UMZC 2015.35.

Description. This genus is represented by a single, well-rolled specimen. The tooth crown consists of a central triangular cusp. This is strongly labio-lingually compressed and lingually inclined. The main cusp is joined at the base to two lateral blades; these are similarly triangular and laterally compressed but slightly smaller than the main cusp. One of the lateral blades has been fractured. The fractured blade reveals that the pulp cavity extends into the lateral blades. The junction of the main cusp and the blades is smooth and slightly concave. A basal flange projects opposite the main cusp. The basal flange is also triangular, but is more obtuse in angle than the cusp or blades. It is also laterally compressed but, due to wear, it is difficult to determine at what point the labial projection of the cusp meets the labial face of the base of the tooth, which projects labially. The crown meets the base at a neck showing six foramina in the lingual view. The angle between the base and the crown is approximately 35°. In basal view the base has two large foramina in lingual-labial positions. The base is laterally 1.8mm long and is twice as deep as it is wide (labio-lingually).

Remarks. Although the angle between the crown and the base is low for the usual range of *Cooleyella*, the base is badly worn at the basal end in particular; this will produce a bias for a smaller angle measurement, as the crown will appear less inclined in relation to the base. We consider this tooth to belong to *Cooleyella* genus, but the worn nature of the tooth precludes species level identification and so we leave this tooth in open nomenclature. This is the earliest record of *Cooleyella*, extending the range from Carboniferous, Viséan–Permian, Cisuralian to Carboniferous, Tournaisian–Cisuralian, Permian.

3.3. Dermal denticles and fin spines

Subclass Elasmobranchii Bonaparte, 1838
Order Ctenacanthiformes Glikman, 1964
Family Ctenacanthidae Dean, 1909
Ctenacanth-type dermal denticle
(Fig. 7a)

Material. UMZC 2015.45.

Description. A dermal denticle showing possible wear of the abraded edges of the base. The base is thick and oval in dorsal view, with a convex basal surface. The neck is wide but defined and the crown of the denticle is tall and slightly irregularly

https://doi.org/10.1017/S1755691018000166 Published online by Cambridge University Press

pointed as it is formed from an amalgamation of flame shaped lobes. The lobes all lean toward the long axis of the base. The crown is oval and similar in outline to the base in dorsal view.

Remarks. The pitted texture may indicate some chemical dissolution, possibly as a result of contact with digestive fluids, or of taphonomic decay such as contact with acidic groundwater.

Ctenacanth-type dermal denticle
(Fig. 7b)

Material. UMZC 2015.44.

Description. A dermal denticle. The base is thin and roughly oval. The neck is thin, well defined and set on the base close to one long edge. The crown is wide and club-like. It leans towards, and overhangs, the long edge to which the neck is set close. Like UMZC 2015.45, the crown is striated and seems to be an amalgamation of lobes.

Order Hybodontiformes Maisey, 1975
Hybodontiformes fin spines
(Fig. 7c–d)

Material. UMZC 2015.46 (Fig 7c). UMZC 2015.47 (Fig 7d).

Description. Fin spine fragment (UMZC 2015.46; Fig. 7c) reconstructed from smaller fragments. This fragment consists of the two posterior edges of the fin spine joined by a concave surface. Both edges are topped by a row of denticles. A spacing of 3 mm between the denticle rows is indicated by the most well preserved and easily assembled fragments, as is the direction of the base concurrent with the widening end. Each denticle is oval and inclined gently toward the base of the spine. The fragmented surface includes two small lines of the interior tissue which extended into the posterior edges. This tissue is heavily vascularised, showing hollow tubes arranged longitudinally. No costae are seen on the tiny and badly damaged fragments of spine wall that are preserved.

The second fin spine (UMZC 2015.47; Fig. 7d) fragment is straight and measures 104 mm in length. The distal tip is missing, either as a result of post-mortem fracture and wear, or wear during life. Most of the base of the fin spine is inaccessible within a very large block of matrix; however, a small portion of the base is on the removed specimen and can be seen on the micro-CT scan. A transverse fracture halfway up the spine exposes the cross-section. The shape of the cross-section, perpendicular to the long axis, is oval, with a concave (assumed) posterior edge formed by a longitudinal groove. The two posterior edges on either side of this concavity are unequal in size, due to taphonomic distortion. The spine has no enameloid outer layer, but is composed of two layers, an outer trabeculine layer and an inner lamellar layer. The outer trabeculine layer has numerous canals running longitudinally. These can be seen in cross-section and cropping out on the surface of the spine to form a striated and pitted texture. The canals in this layer tend to remain open around the outer surface of the spine, but are infilled towards the middle of the spine so that only a smooth surface with polygonal demarcations between old canals can be seen. A large and triangular mesial canal sits within this outer layer at the mesial edge of the spine. It is 1.5 mm across at this point and infilled with sediment. This mesial canal runs the length of the spine and is visible from the exterior in places where the mesial edge of the spine is fractured. The inner lamellar layer comprises most of the area of the spine's cross-section. The centre of the layer is deposited to form concentric ovals, towards the outside of the layer the concentric circles are folded to form irregular wave-like projections, further towards the outside the lamellar structure becomes invisible and the layer is homogeneous. A relatively small y-shaped pulp cavity sits posterior to the middle of the concentric circles and is infilled in the same manner as the mesial canal. The micro-CT scans are not able to show high-quality histological detail; however, it is clear that both layers observed at the middle of the spine extend right to the spine tip and also down to, at least, the start of the obliquely fractured basal area of the spine. At this point, the spine is heavily recrystallised with high density minerals which obscure histological details in the scan. It is not clear how the pulp cavity changes shape through the spine from scan details. No costae can be seen on this spine, probably due to the loss of the outer layer which would have carried them, if present.

Remarks. UMZC 2015.47 is similar to those of hybodontiform sharks in the oval cross-section with two posterior projecting ridges, separated by a concave groove, in the separation between an inner lamellar layer and an outer trabeculine layer and in the likely presence of a large mesial canal. In hybodontiforms the posterior ridges bear hooked denticles. It is possible that an exterior ornamented layer has been lost from UMZC 2015.47 through taphonomic wear, a theory supported by the spine's deformation and the heavily fractured state of the mesial edge, the base and possibly the tip. Additionally, the presence of UMZC 2015.46 indicates that 'delamination' of the ornamented layer, is possible at this site. It is possible that UMZC 2015.46 is a fragment of the enameloid layer of this large fin spine. The interior vascularised tissue seen on the reverse of the denticled surface corresponds to the trabecular dentine in the UMZC 2015.47. The 3-mm gap between the denticle rows matches that of the distal region of the UMZC 2015.47 and supports a conspecific origin. Additionally, in this case wear would have removed the sharp downcurved tips of the posterior denticles to form rounded and down-leaning denticles similar to those observed in this specimen. Maisey (1977, 1978) notes that the lamellar dentine of hybodontiforms is discontinued distal of the base, although thin sectioning of modern embryonic holocephalan fin spines (Jerve *et al*. 2014) indicates that very thin lamellar layers may be difficult to see in the adult morphology, despite being clear at embryonic stages. Due to preservational artefacts, we cannot tell if both histological layers continue down into the base in UMZC 2015.47.

4. Discussion

4.1. Whitrope Burn chondrichthyans

This study has recovered 57 whole or almost whole teeth, and hundreds of worn or fractured teeth that could not be reliably identified. The 57 specimens resulted in the identification of 21 tooth taxa from Whitrope Burn. One spine taxon and one dermal denticle taxon were identified. The teeth are found in concentrations alongside fragments of actinopterygian teeth, scales and bone, tetrapod bone, rhizodont bone, lungfish tooth plates and shelly fragments. Teeth range in preservation from very well-preserved to abraded and fractured. We are able to identify 11 of the 20 tooth taxa to generic level (see Table 1), one is identified to species level and two are assigned to new species. Of the remaining seven genera identified, five (*Harpagofututor*, *Deihim*, *Protacrodus*, *Deltodus, Platyxystrodus*) may be new species, but are represented by only one or two teeth and so are left in open nomenclature; the remaining two (*Cooleyella*, *Cladodus*) are too badly preserved to identify beyond generic level.

https://doi.org/10.1017/S1755691018000166 Published online by Cambridge University Press

Table 1 Taxon counts of whole or almost whole Whitrope Burn chondrichthyan fossils. Includes both UMZC and NMS specimens

Taxon	No. of specimens identified
?Helodus simplex	1
?Helodontidae indet. 1	2
?Helodontidae indet. 2	12+
Harpagofututor sp.	1
Platyxystrodus waverleyi sp. nov.	3
Psephodontidae indet. 1	4+
Psephodontidae indet. 2	1
Psephodontidae indet. 3	1
Whitropus longicalcus gen. nov. sp. nov.	10+
Deltodus tubineus sp. nov.	4
Deltodus sp.	2+
Cochliodontiformes indet. 1	1
Holocephali indet. 1	2+
Holocephali indet. 2	1
Holocephali indet. 3	1+
Cladodus sp.	2+
Protacrodus sp.	1
Deihim sp.	1
Protacrodontidae indet.	1
Cooleyella sp.	1
Ctenacanth-type dermal denticles	3+
Hybodontiform fin spine	2

This makes this the second most diverse sample of Tournaisian chondrichthyans anywhere in the world, behind the Avon Gorge Black Rock Limestone (Stoddart 1875). The Whitrope Burn fauna, as sampled here, comprises 16 holocephalans and seven elasmobranchs and is dominated by crushing dentitions. Holocephalan diversity is not dominated by any one family, but consists of helodontids, cochliodontids, psephodontids, chondrenchelyids and unidentified holocephalans. Most of these taxa are identifiable to some level, but cannot be identified to species or even genus level. In most cases, this is because too few complete specimens are available to provide a good study of intraspecific variation. They do indicate, however, that the individual taxa are not those seen in other Tournaisian UK sites, but are rather suggestive of some degree of endemism.

Elasmobranch diversity is lower and more cosmopolitan and consists of *Cladodus*, three protacrodontids, *Cooleyella* and a hybodont. *Cladodus* is common in other Tournaisian sites (e.g., Stoddart 1875; Roelofs *et al*. 2016) as it is here. Of the protacrodontids, *Protacrodus* is also found in other Tournaisian sites, including China (Ginter & Sun 2007), Australia (Roelofs *et al*. 2016), Iran (Habibi & Ginter 2011), the south Urals (Ivanov 1996), Ireland (Duncan 2006) and Cromhall Quarry (Behan *et al*. 2012), although not in the Avon Gorge faunas, possibly due to a lack of the micro-faunal sampling needed to detect this small tooth. *Deihim* is also found in the Upper Devonian of Iran (Hairapetian & Ginter 2009), Morocco (Ginter *et al*. 2002) and Armenia (Ginter *et al.* 2002); the Whitrope Burn tooth probably represents a new species. *Cooleyella* is widespread geographically and temporally and is known from the Viséan of the UK (Duffin & Ward 1983) to the Cisuralian of the USA and Russia (Duffin & Ward 1983; Ivanov 2000, 2005). We can extend the occurrence of *Cooleyella* in the UK, from the Viséan, back to the Tournaisian.

4.2. Palaeoenvironment

Geological analysis of the Whitrope Burn chondrichthyan dolostone (bed 6) indicates deposition of a mixture of carbonate and siliclastic sediment and fossils from a high-density turbidity current on a marine shelf. The absence of any wave-produced structures indicates deposition below wave base. The fossils originated in an environment that was probably near-shore, as suggested by the presence of tetrapod skeletal elements and large numbers of strap-like plant leaves. Analysis of the beds surrounding the fossiliferous bed suggests a marine setting, where initially high carbonate production was eventually replaced by an increasingly dominant fine-grained siliciclastic input. The micaceous siltstones overlying beds 1–7 indicate that carbonate production had largely ceased.

This study notes the presence of a diverse chondrichthyan fauna, *Cavellina* ostracods and *Naiadites* bivalves as rare evidence of a marine influence in the Ballagan Formation. The Whitrope Burn Ballagan may represent a lagoonal environment, or the incursion of the Northumberland basin marine environment (Stone *et al*. 2010). The faunal data show that the majority of the chondrichthyans in Whitrope Burn were durophagous and likely to be largely demersal. Very few of the taxa present were likely to be pelagic, open-water chondrichthyans or have demonstrated large geographical ranges in the Tournaisian; the notable exception being *Cladodus*, although both *Deihim* and *Cooleyella* achieved this status to some degree in the Upper Devonian and Viséan, respectively. This suggests that the environment was not unrestricted marine shelf but a sheltered lagoon or bay with restricted access.

4.3. A diverse post-Hangenberg fauna

We have evidence of several UK Tournaisian environments with rich and varied faunas. The Avon Group sites are Courceyan (Hastarien–Ivorian) and the chondrichthyans there are overwhelmingly represented by large crushing teeth, with very few high-cusped teeth reported (Stoddart 1875), although several rare *Cladodus* teeth reach a large size of approximately 4 cm tooth height. The Black Rock Limestone in Bristol (BRL) and at Cromhall Quarry may include the lower Viséan, as its deposition covers a Courceyan–Chadian timespan (Waters *et al*. 2011; Behan *et al*. 2012). The Bristol BRL fauna is still, like the Avon Group, dominated by durophagous holocephalans. The Cromhall Quarry fauna is dominated by relatively small piscivorous and durophagous elasmobranchs, with few large durophagous holocephalan taxa. The Whitrope Burn Ballagan fauna shares similarities with both. The fauna is dominated by durophagous holocephalans, but there is also evidence of large and small elasmobranch teeth that are less strongly durophagous. The Whitrope Burn Ballagan fauna does differ from the Cromhall fauna in the lack of specialised-piscivorous teeth. The Cromhall fauna may be Viséan in age, so it is uncertain whether the faunal differences are due to a temporal shift in the fauna. Alternatively, it may simply be an environmental effect indicating high beta diversity, possibly driven by niche specialisation or by the exclusion of open water chondrichthyans such as *Stethacanthus* and *Thrinacodus* by a closed lagoonal habitat. It is likely that the Avon Gorge Black Rock Limestone fauna is influenced by a collection bias toward large holocephalan teeth, a speculation supported by the presence in collections of very large *Cladodus* and *Helodus* teeth, and that it could yield chondrichthyan microfossils representing a missing elasmobranch fauna.

The low number of diverse Tournaisian sites in the UK and the neglected state of Carboniferous chronostratigraphy preclude detailed statistical tests of biodiversity at this stage. However, a previous study of the Avon Gorge Tournaisian limestone provides preliminary evidence of biodiversity changes through the Tournaisian–Viséan sequences. Stoddart (1875) gathered complete faunal lists from two successions of limestones; the Courceyan Avon Group and the Courceyan–Chadian Black Rock Limestone (BRL) Subgroup. His results are summarised in Table 2. These results must be treated cautiously,

https://doi.org/10.1017/S1755691018000166 Published online by Cambridge University Press

Table 2 Summary of fossil distribution in the Avon Gorge limestones as recorded by Stoddart (1875). The term non-chondrichthyan represents a range of invertebrates and one actinopterygian

	Total fauna	Chondrichthyan	Non-chondrichthyan
Sum all taxa	102	24	78
Sum Avon Group taxa	56	8	48
Sum Avon Group taxa/unit thickness (95.4 m)	0.59	0.084	0.5
Sum BRL Subgroup	57	24	33
Sum BRL Subgroup taxa/unit thickness (349.3 m)	0.16	0.069	0.094
Overlap	11	8	3
Avon Group unique taxa	45	0	45
BRL Subgroup unique taxa	46	16	30

further work is needed to establish which of Stoddart's specimens are those referred to in his published faunal lists. However, we think that the list, as published, is a rudimentary but valuable, account of biodiversity through the Avon Gorge Limestones, and is adequate for low resolution biodiversity comparisons across space and time.

These diversity counts highlight two points. Firstly, all eight chondrichthyans found in the Avon Group are also found in the BRL Subgroup; 33 % of all chondrichthyan taxa are present in both units. In the non-chondrichthyan taxa, only three of the 48 taxa found in the Avon Group are also found in the BRL Subgroup; only 6 % of all non-chondrichthyan taxa are present in both units. Secondly, the diversity of the chondrichthyan fauna increases from the Avon Group to the BRL Subgroup, but the diversity of the non-chondrichthyan fauna decreases. The chondrichthyan sum taxon count increases by 300 %. The non-chondrichthyan sum taxon count decreases by 31 %. A rock bias is likely in this case, as the number of beds in the two categories is similar (14 for the Avon Group, 13 for the BRL Subgroup) but the sequence of the BRL Subgroup is much larger, an approximate calculation from original bed measurements indicate that the Avon Group is represented by 95.4 m and the BRL Subgroup by 349.3 m. This would tend to give falsely diverse faunas in the BRL. However, we consider bed number to be more important factor in diversity than bed thickness, as each bed represents a different time or environment, whereas a single bed, no matter how thick it is, is much more likely to represent a single fauna when reworking is taken into account.

In summary, this sample suggests that the largely invertebrate fauna undergoes a substantial faunal turnover and small decrease in diversity, with very few taxa occurring through the Avon Gorge units. In contrast, chondrichthyans increase in diversity through the Avon Gorge units with no loss of any taxa. This is a pattern that we might expect to see in an area with shifting environmental parameters, where sessile invertebrates suffer local extinction and faunal turnovers but mobile and predatory vertebrates are able to escape inimical conditions and thrive on a variety of prey. The increase in chondrichthyan diversity may be the result of a local environmental change. Alternatively, given the motile lifestyle of large marine vertebrates it may provide evidence for wide-scale recovery and diversification following the Hangenberg extinction event (HEE).

The Whitrope Burn Ballagan is currently thought to represent a late Tournaisian to early Viséan site and so, along with the Black Rock Limestone, adds to evidence of high chondrichthyan diversity around the end of the Tournaisian. Evidence from UK and Irish localities spanning the Tournaisian suggests that these areas were dominated by durophagous holocephalans, whereas this pattern has yet to be shown so clearly in the American, Russian, European, Australian and Chinese faunas. Within the UK, the chondrichthyan fauna at later sites spanning the Tournaisian and Viséan are less dominated by holocephalans, instead elasmobranchs are dominant in both non-crushing and crushing niches (e.g., Behan *et al.* 2012; Ginter *et al.* 2015; Richards 2016). This points to a complex picture in which crushing chondrichthyan diversity is controlled by spatial shifts in niche availability over time. The lagoonal habitat represented by Whitrope Burn may represent a temporary refugium which is host to a near-relict fauna dominated by large crushing holocephalan chondrichthyans. Many of these had already become scarce in other localities and become extinct later in the Carboniferous.

Our results neither support nor refute the presence of a post-HEE trough across all chondrichthyans worldwide, as the date of Whitrope Burn is likely to be too young to be applicable. The sample does show, however, that long-term faunal changes are likely to occur at different rates in different environments, providing incongruous results between geographically close localities. This suggests that the effect of the HEE on chondrichthyans may have been geographically and biologically (phylogenetically and morphologically) heterogeneous.

4.4. A durophagous post-Hangenberg fauna

The crowns of the elasmobranch cusps are tall in relation to the width compared to the holocephalan toothplates, but all of these cusp types are robust and there is evidence from biomechanical experiments (Whitenack & Motta 2010; Whitenack *et al.* 2011) that all of the teeth represented at Whitrope Burn would probably have been capable of accessing hard-shelled prey items, as well as evidence from bite marks (Mapes & Hansen 1984) and stomach contents (Williams 1990) that suggest that they actually did. The micro-faunal assemblage at Whitrope Burn is dominated by protacrodonts, like those seen at Cromhall Quarry and at the Mobarak Formation in Iran. The macro-faunal assemblage, however, represents a diverse holocephalan fauna similar to that in evidence in the Avon Group beds of Bristol. Whitrope Burn is the first UK Tournaisian site where strong evidence is found of these two faunas sharing an environment. High durophagy levels in Tournaisian chondrichthyans mirror observations of durophagy in concurrent actinopterygians and sarcopterygians (Sallan & Coates 2013). It also concurs with evidence of increased shell predation in the Mississippian (Salamon *et al.* 2014).

The abundant crushing-predator presence in the early Tournaisian is supported by patterns of crinoid evolution, namely a decline in camerate crinoids vulnerable to crushing and a subsequent faunal turnover. This is likely to have been driven by predation pressure rather than by predation release (Sallan *et al.* 2011).

The dating of Whitrope Burn is crucial to understanding whether the radiation of durophagous chondrichthyans took place immediately after the end-Devonian mass extinction or whether a post-extinction trough occurs. The Whitrope Burn Ballagan is dated to the latest Tournaisian or earliest Viséan.

https://doi.org/10.1017/S1755691018000166 Published online by Cambridge University Press

Durophagy in chondrichthyans during the Tournaisian is noted by Sallan *et al*. (2011, p. 8337) who say that "Crushers represent 57 % (40 of 71) of all chondrichthyans by the end of the Tournaisian *vs*. 21 % (8 of 37) of the Famennian shark fauna". We agree with another observation (Sallan & Coates 2010), which is that low overall diversity at the base of the Tournaisian may be due to undersampling. Our diversity count of the Courceyan (Lower Tournaisian) Avon Group beds reveals the most diverse Tournaisian chondrichthyan assemblage in the world. Our data suggest that with increased sampling of Lower and Middle Tournaisian beds, a high diversity of 'crushers' would be seen here too.

5. Conclusions

The Whitrope Burn fauna represents a diverse marine assemblage of holocephalan and elasmobranch chondrichthyans from the latest Tournaisian to earliest Viséan. The teeth, dermal denticles and fin spines were transported, and possibly concentrated, as part of a density current deposit from a near shore environment. We suggest that the Whitrope Burn site was a marine lagoon or bay with spatially or temporally restricted access to open marine shelf. This is based on the combined geological and invertebrate palaeontological evidence for a marginal-marine lagoon or relatively brief marine incursion, coupled with the presence of a diverse and locally unique holocephalan faunal assemblage but a much more cosmopolitan elasmobranch assemblage. The chondrichthyan fauna is characterised by durophagous dentitions and a range of tooth sizes, including holocephalan teeth much larger than their later Viséan postcedents.

This fauna adds to growing, multi-faunal evidence from localities worldwide that the chondrichthyan fauna following the Hangenberg extinction event is diverse and dominated by durophagous dentitions. Further chondrichthyan work is needed to correct the undersampling bias observed at the base of the Tournaisian and, also, to constrain the temporal framework of existing Tournaisian sites in order to understand in greater detail the timing, pattern and extent of the chondrichthyan radiation.

6. Author contributions

TRS and JAC collected material from Whitrope Burn in 2006. TRS, RFB and KRR collected material and JES logged Whitrope Burn and collected geological and palynological samples in 2014. KRR, TRS and RFB prepared palaeontological material. KRR visited museums, took photographs and prepared and rendered micro-CT scans. JES prepared geological material and JES and SJD analysed geological material. JEAM conducted the palynological analysis.

7. Acknowledgements

The sites along the Whitrope and Roughley Burns, and much of the material described above, were discovered by the late Stan Wood, and it is a pleasure to acknowledge the enormous contribution he made to our understanding of Early Carboniferous sharks. We thank Stig Walsh (NMS) and Maggie Wood for the loan of specimens; Claudia Hildebrandt (University of Bristol), Daniel Pemberton and Matthew Riley (Sedgwick Museum, Cambridge) and Matthew Lowe (UMZC) for access to specimens under their care; Sarah Exton and the Buccleuch Estate for permission to collect along the Whitrope and Roughley Burns; Keturah Smithson (UMZC) for micro-CT scanning; Sarah Finney (Sedgwick Museum, Cambridge) for the loan of equipment; the British Geological Survey (BGS) for access to unpublished geological maps; Peter Brand (BGS) and Carys Bennett (UoL) for help in identifying the fossil invertebrates; and Mike Coates (University of Chicago) for helpful discussion. We are particularly grateful to the Referees, Michal Ginter and Chris Duffin, for their detailed reviews of the manuscript which significantly improved the paper.

This is a contribution to the TW:eed Project, 'Tetrapod World: early evolution and diversity', and is also a contribution to IGCP Project 596, 'Climate change and biodiversity patterns in the mid-Palaeozoic'. This work was carried out with the aid of NERC research grants NE/J022713/1 (Cambridge), NE/J020729/1 (Leicester) and NE/J021091/1 (Southampton), and funding support from the John Ray Trust, Queens College, Cambridge and the J. Arthur Ramsey Fund.

8. References

Agassiz, L. 1838. *Recherches sur les Poisons Fossiles.* Volume 3. Neuchâtel, Switzerland: Petitpierre.

Agassiz, L. 1843. *Recherches sur les Poisons Fossiles.* Volume 5. Neuchâtel, Switzerland: Petitpierre.

Behan, C., Walkden, G. & Cuny, G. 2012. A Carboniferous chondrichthyan assemblage from residues within a Triassic Karst system at Cromhall Quarry. *Palaeontology* **55**, 1245–63.

Bennett, C. E., Siveter, D. J., Davies, S. J., Williams, M., Wilkinson, I. P., Browne, M. & Miller, C. G. 2012. Ostracods from freshwater and brackish environments of the Carboniferous of the Midland Valley of Scotland: the early colonization of terrestrial water bodies. *Geological Magazine* **149**, 366–96.

Berg, L. S. 1940. Sistema ryboobraznykh i ryb, nyne zhivushchikh i iskopaemykh. [Classification of fishes, both recent and fossil]. *Trudy Zoologicheskogo Instituta Akademii Nauk SSSR* [Proceedings of the Zoological Institute, USSR Academy of Sciences] **5**, 1–517.

Bonaparte, C. L. 1831. Saggio di una distribuzione metodica degli animali vertebrati. *Giornale Arcadico di Scienze* **49**, 1–77.

Bonaparte, C. L. 1838. Selachorum tabula analytica. *Nuovi Annali delle Scienze Naturali (Bologna)* **1**, 195–214.

Brandon, A., Riley, N. J., Wilson, A. A. & Ellison, R. A. 1995. Three new early Namurian (E_{1c}–E_{2a}) marine bands in central and northern England, UK, and their bearing on correlations with the Askrigg Block. *Proceedings of the Yorkshire Geological Society* **50**, 333–35.

Bromley, R. G. 1996. *Trace fossil: biology, taphonomy and applications.* London: Chapman & Hall. 378 pp.

Capetta, H., Duffin, C. J. & Zidek, J. 1993. Chondrichthyes. *In* Benton, M. J. (ed.) *The Fossil Record*, Vol 2, 593–609. London: Chapman & Hall. xviii + 846 pp.

Compagno, L. J. V. 1977. Phyletic Relationships of Living Sharks and Rays. *American Zoologist.* **17**, 303–22.

Davis, J. W. 1883. On the fossil fishes of the Carboniferous limestone series of Great Britain. *Scientific Transactions of the Royal Dublin Society* **1**, 327–600.

Dean, B. 1909. Studies on fossil fishes (sharks, chimaeroids, and arthrodires). *Memoirs of the American Museum of Natural History* **9**, 211–87.

Duffin, C. J. & Ginter, M. 2006. Comments on the Selachian Genus "Cladodus" Agassiz, 1843. *Journal of Vertebrate Paleontology* **26**, 253–66.

Duffin, C. J. & Ward, D. 1983. Neoselachian sharks' teeth from the Lower Carboniferous of Britain and the Lower Permian of the USA. *Palaeontology* **26**, 93–110.

Duncan, M. 2003. Early Carboniferous chondrichthyan *Thrinacodus* from Ireland, and a reconstruction of jaw apparatus. *Acta Palaeontological Polonica* **48**, 113–22.

Duncan, M. 2004. Chondrichthyan genus *Lissodus* from the Lower Carboniferous of Ireland. *Acta Palaeontologica Polonica* **49**, 417–28.

Duncan, M. 2006. Various chondrichthyan microfossil faunas from the Lower Mississippian (Carboniferous) of Ireland. *Irish Journal of Earth Sciences* **24**, 51–69.

Edwards, W. & Stubblefield, C. J. 1947. Marine bands and other faunal marker-horizons in relation to the sedimentary cycles of the middle coal measures of Nottinghamshire and Derbyshire. *Quarterly Journal of the Geological Society* **103**, 209–56.

Finarelli, J. A. & Coates, M. I. 2014. *Chondrenchelys problematica* (Traquair, 1888) redescribed: a Lower Carboniferous, eel-like holocephalan from Scotland. *Earth and Environmental Science Transactions of the Royal Society of Edinburgh* **105**, 35–59.

Garvey, J. & Turner, S. 2006. Vertebrate remains from the presumed earliest Carboniferous of the Mansfield Basin, Victoria. *Alcheringa* **30**, 43–62.

Ginter, M. 1999. Famennian-Tournaisian chondrichthyan microremains from the eastern Thuringian Slate Mountains. *Abhandlungen und Berichte für Naturkunde, Magdeburg* **21**, 25–47.

Ginter, M., Hairapetian, V. & Klug, S. 2002. Famennian chondrichthyans from the shelves of North Gondwana. *Acta Geologica Polonica* **52**, 169–215.

Ginter, M., Hampe, O. & Duffin, C. J. 2010. Chondrichthyes. Paleozoic Elasmobranchii: teeth. *In* Schultze, H-P. (ed.) *Handbook of Paleoichthyology*, Volume 3D. München: Verlag Dr. Friedrich Pfeil. 512 pp.

Ginter, M., Duffin, C. J., Dean, M. T. & Korn, D. 2015. Late Viséan pelagic chondrichthyans from northern Europe. *Acta Palaeontologica Polonica* **60**, 899–922.

Ginter, M. & Sun, Y. 2007. Chondrichthyan remains from the Lower Carboniferous of Muhua, southern China. *Acta Palaeontologica Polonica* **52**, 705–27.

Glikman, L. S. 1964. *Akuly paleogena I ih stratigrafičeskoe značenie* [*Sharks of the Paleogene and their stratigraphic significance*]. Moscow: Doklady Akademii Nauk SSSR [Academy of Sciences of the USSR].

Gunnell, F. H. 1933. Conodonts and fish remains from the Cherokee, Kansas City, and Wabaunsee Groups of Missouri and Kansas. *Journal of Paleontology* **7**, 261–97.

Habibi, T. & Ginter, M. 2011. Early Carboniferous chondrichthyans from the Mobarak Formation, central Alborz Mountains, Iran. *Acta Geologica Polonica* **61**, 27–34.

Hairapetian, V. & Ginter, M. 2009. Fammenian chondrichthyan remains from the Chariseh section, Central Iran. *Acta Geologica Polonica* **59**, 173–200.

Hay, O. P. 1899. On some changes in the names, generic and specific, of certain fossil fishes. *American Naturalist* **33**, 783–92.

Hay, O. P. 1902. Bibliography and catalogue of the fossil vertebrata of North America. *Bulletin of the United States Geological Survey* **179**, 1–868.

Huxley, T. H. 1880. On the application of the laws of evolution to the arrangement of the Vertebrata, and more particularly of the Mammalia. *Proceedings of the Zoological Society of London* **43**, 649–62.

Ivanov, A. O. 1996. The Early Carboniferous chondrichthyans of the South Urals, Russia. *Geological Society, London, Special Publications* **107**, 417–25.

Ivanov, A. 2000. Permian elasmobranchs (Chondrichthyes) of Russia. *Ichthyolith Issues, Special Publication* **6**, 39–42.

Ivanov, A. 2005. Early Permian Chondrichthyans of the Middle and South Urals. *Revista Brasileira de Paleontologia* **8**, 127–38.

Jaekel, O. 1925. Das Mundskelett der Wirbeltiere. *Gegenbaurs Morphologisches Jahrbuch* **55**, 402–09.

Jerve, A., Johanson, Z., Ahlberg, P. & Boisvert, C. 2014. Embryonic development of fin spine in *Callorhincus milii* (Holocephali); implications for chondrichthyan fin spine evolution. *Evolution & Development* **16**, 339–53.

Kriwet, J., Kiessling, W. & Klug, S. 2009. Diversification trajectories and evolution life-history traits in early sharks and batoids. *Proceedings of the Royal Society, London, Series B* **276**, 945–51.

Lebedev, O. A. 1996. Fish assemblages in the Tournaisian–Viséan environments of the East European Platform. *Geological Society, London, Special Publications* **107**, 387–415.

Lund, R. 1982. *Harpagofututor volsellorhinus* New genus and species (Chondrichthyes, Chondrenchelyiformes) from the Namurian Bear Gulch Limestone, *Chondrenchelys problematica* Traquair (Viséan), and their sexual dimorphism. *Journal of Paleontology* **56**, 938–58.

Lund, R. & Grogan, E. D. 1997. Relationships of the Chimaeriformes and the basal radiation of the Chondrichthyes. *Reviews in Fish Biology and Fisheries* **7**, 65–123.

Maisey, J. G. 1975. The interrelationships of the phalacanthous selachians. *Neues Jahrbuch für Geologie und Paläontologie* **9**, 553–67.

Maisey, J. G. 1977. The fossil selachian fishes *Palaeospinax* Egerton, 1872 and *Nemacanthus* Agassiz, 1837. *Zoological Journal of the Linnean Society* **60**, 259–73.

Maisey, J. G. 1978. Growth and form of finspines in hybodont sharks. *Palaeontology* **21**, 657–66.

Manski, C. F. & Lucas, S. G. 2013. Romer's Gap Revisited: Continental Assemblages and Ichno-assemblages from the basal Carboniferous of Blue Beach, Nova Scotia, Canada. The Carboniferous–Permian Transition. *Bulletin of the New Mexico Museum of Natural History and Science* **60**, 244–73.

Mapes, R. H. & Hansen, M. C. 1984. Pennsylvanian shark-cephalopod predation: a case study. *Lethaia* **17**, 175–83.

McCoy, F. A. 1855. *A Systematic description of the British Palaeozoic fossils in the Geological Museum of the University of Cambridge*. 1–661.

McKenzie, M. A. & Bamber, E. W. 1979. An occurrence of Lower Carboniferous fish remains from Alberta, Canada. *Canadian Journal of Earth Sciences* **16**, 1628–31.

Morris, J. & Roberts, G. E. 1862. On the Carboniferous limestone of Oreton and Farlow, Clee Hills, Shropshire. *Quarterly Journal of the Geological Society of London* **18**, 94–106.

Newberry, J. S. & Worthen, A. H. 1866. Descriptions of new species of vertebrates, mainly from the Sub-Carboniferous Limestone and Coal Measures of Illinois. *Geological Survey of Illinois* **2**, 9–134.

Newberry, J. S. & Worthen, A. H. 1870. Geology and Paleontology. Descriptions of fossil vertebrates. *Geological Survey of Illinois* **4**, 343–74.

Obruchev, D. V. 1953. Lzuchenie edestid y raboty A. P. Karpinskogo [Studies on edestids and the works of A. P. Karpinski]. *Trudy Paleontologièeskog Instituta Akademii Nauk SSSR* [*Proceedings of the Paleontological Institute, USSR Academy of Sciences*] **45**, 1–85.

Owen, R. 1867. On the dental characters of genera and species, chiefly of fishes from the Low Main Seam and shales of coal, Northumberland. *Transactions of the Odontological Society of Great Britain* **5**, 329–34.

Patterson, C. 1965. The phylogeny of chimaeroids. *Philosophical Transactions of the Royal Society, London, Series B* **249**, 101–219.

Patterson, C. 1992. Interpretation of the toothplates of chimaeroid fishes. *Zoological Journal of the Linnean Society* **106**, 33–61.

Pemberton, S. G., Spila, M., Pulham, A. J., Saunders, T., MacEachern, J. A., Robbins, D. & Sinclair, I. K. 2001. Ichnology and sedimentology of shallow to marginal marine systems: Ben Nevis & Avalon reservoirs, Jeanne D'Arc Baisin. *Geological Association of Canada, Short Course Notes* **15**. St Johns, Newfoundland: Geological Association of Canada. 343 pp.

Richards, K. R. 2016. *Carboniferous chondrichthyans from the Derbyshire limestones*. Doctoral Thesis, University of Cambridge. 326 pp.

Roelofs, B., Barham, M., Mory, A. J. & Trinajstic, K. 2016. Late Devonian and Early Carboniferous chondrichthyans from the Fairfield Group, Canning Basin, Western Australia. *Palaeontologia Electronica* **19**, 1–28.

Salamon, M. A., Gorzelak, P., Niedźwiedzki, R., Trzęsiok, D. & Baumiller, T. K. 2014. Trends in shell fragmentation as evidence of mid-Paleozoic changes in marine predation. *Paleobiology* **40**, 14–23.

Sallan, L. C., Kammer, T. W., Ausich, W. I. & Cook, L. A. 2011. Persistent predator–prey dynamics revealed by mass extinction. *Proceedings of the National Academy of Sciences USA* **108**, 8335–38.

Sallan, L. C. & Coates, M. I. 2010. End-Devonian extinction and a bottleneck in the early evolution of modern jawed vertebrates. *Proceedings of the National Academy of Sciences USA* **107**, 10131–35.

Sallan, L. C. & Coates, M. I. 2013. Styracopterid (Actinopterygii) ontogeny and the multiple origins of post-Hangenberg deep-bodied fishes. *Zoological Journal of the Linnean Society* **169**, 156–99.

Schram, F. R. 1979. British Carboniferous Malacostraca. *Fieldiana Geology* **40**, 1–129.

Smithson, T. R., Richards, K. R. & Clack, J. A. 2015. Lungfish diversity in Romer's Gap: reaction to the end-Devonian extinction. *Palaeontology* **59**, 29–44.

Stahl, B. J. 1999. Chondrichthyes III. Holocephali, *In* Schultze, H-P. (ed.) *Handbook of Paleoichthyology*, Volume 3. München: Verlag Dr. Friedrich Pfeil.

St John, O. H. & Worthen, A. H. 1875. Descriptions of fossil fishes. *Geological Survey of Illinois* **6**, 245–488.

St John, O. H. & Worthen, A. H. 1883. Descriptions of fossil fishes; a partial revision of the Cochliodonts and Psammodonts. *Geological Survey of Illinois* **7**, 55–264.

Stoddart, W. W. 1875. The Geology of the Bristol coal-field. *Proceedings of the Bristol Naturalist's Society* **1**, 115–40.

Stone, P., Millward, D., Young, B., Merritt, J. W., Clarke, S. M., McCormac, M. & Lawrence, D. J. D. 2010. *British Regional Geology: Northern England* (Fifth edition). Keyworth, Nottingham, UK: British Geological Survey.

Turnau, E., Avchimovitch, V.I., Byvsheva, T. V., Carson, B., Clayton, G. & Owens, B. 1997. The first appearance in Europe of *Lycospora pusilla* (Ibrahim) Somers and its relationship to the Tournaisian/

Viséan boundary. *Prace Państwowego Instytutu Geologicznego* **157**, 289–93.
Turner, S. 1982. Middle Palaeozoic elasmobranch remains from Australia. *Journal of Vertebrate Paleontology* **2**, 117–31.
Turner, S. 1991. Palaeozoic vertebrate microfossils of Australia. *In* Vickers-Rich, P, Monaghan, J. N., Baird, R. F. & Rich, T. H. (eds) *Vertebrate palaeontology of Australasia*, 429–64. Melbourne: Pioneer Design Studios. xvi + 1437 pp.
Turner, S. 1993. Palaeozoic microvertebrates biostratigraphy of Eastern Gondwana. *In* Long, J. A. (ed.) *Palaeozoic vertebrate biostratigraphy and* biogeography, 174–207. London: Belhaven Press. 384 pp.
Underwood, C. J., Mitchell, S. F. & Veltkamp, K. J. 1999. Shark and ray teeth from the Hauterivian (Lower Cretaceous) of northeast England. *Palaeontology* **42**, 287–302.
Waters, C. N., Waters, R. A., Jonas, N. S., Cleal, C. J. & Davies, J. R. 2011. Bristol, Mendips and Forest of Dean. *In* Waters, C. N., Somerville, I. D., Jones, N. S., Cleal, C. J., Collinson, J. D., Waters, R. A., Besly, B. M., Dean, M. T., Stephenson, M. H., Davies, J. R., Freshney, E. C., Jackson, D. I., Mitchell, W. I., Powell, J. H., Barclay, W. J., Browne, M. A. E., Leveridge, B. E., Long, S. L. & McLean, D. (eds) *A revised correlation of Carboniferous rocks in the British Isles. Geological Society of London, Special Report* **26**, 37–43. London & Bath: The Geological Society. 186 pp.
Whitenack, L. B., Simkins, D. C. & Motta, P. J. 2011. Biology meets engineering: the structural mechanics of fossil and extant shark teeth. *Journal of Morphology* **272**, 169–79.
Whitenack, L. B. & Motta, P. J. 2010. Performance of shark teeth during puncture and draw: implications for the mechanics of cutting. *Biological Journal of the Linnean Society* **100**, 271–86.
Williams, M., Leng, M. L., Stephenson, M. H., Andrews, J. E., Wilkinson, I. P., Siveter, D. J., Horne, D. J. & Vannier, J. M. C. 2006. Evidence that Early Carboniferous ostracods colonised coastal flood plain brackish water environments. *Palaeogeography, Palaeoclimatology, Palaeoecology* **230**, 299–318.
Williams, M. E. 1990. Feeding behavior in Cleveland Shale fishes. *In* Boucot, A. J. (ed.) *Evolutionary Paleobiology of Behavior and Coevolution*, 273–87. Amsterdam: Elsevier Science. 725 pp.
Wood, S. P. & Rolfe, W. D. I. 1985. Introduction to the palaeontology of the Dinantian of Foulden, Berwickshire, Scotland. *Transactions of the Royal Society of Edinburgh: Earth Sciences* **76**, 1–6.
Woodward, A. S. 1889. *Catalogue of the fossil fishes in the British Museum (Natural History) Part 1*. London: British Museum (Natural History).
Zangerl, R. 1981. Chondrichthyes I. Paleozoic Elasmobranchii. *In* Schultze, H-P. (ed.) *Handbook of Paleoichthyology*, Vol. 3A. Stuttgart: Gustav Fischer. 115 pp.

MS received 7 December 2015. Accepted for publication 16 October 2017.